

NAVAL POSTGRADUATE SCHOOL

Monterey, California

AD-A205 353



THESIS

COMPUTERIZED MEASUREMENT OF
THERMOACOUSTICALLY GENERATED
TEMPERATURE GRADIENTS

by

MILTON DAVID KITE

December 1988

Thesis Advisor:
Co-Advisor

A. A. Atchley
T. J. Hofler

Approved for public release; distribution unlimited

DTIC
ELECTE
MAR 14 1989
S H D

89 3 14 024

UNCLASSIFIED

SECURITY CLASSIFICATION OF THIS PAGE



REPORT DOCUMENTATION PAGE

1a REPORT SECURITY CLASSIFICATION UNCLASSIFIED			1b RESTRICTIVE MARKINGS		
2a SECURITY CLASSIFICATION AUTHORITY			3 DISTRIBUTION/AVAILABILITY OF REPORT Approved for public release; distribution is unlimited.		
2b DECLASSIFICATION/DOWNGRADING SCHEDULE					
4. PERFORMING ORGANIZATION REPORT NUMBER(S)			5. MONITORING ORGANIZATION REPORT NUMBER(S)		
6a. NAME OF PERFORMING ORGANIZATION Naval Postgraduate School	6b. OFFICE SYMBOL (If applicable) Code 61	7a. NAME OF MONITORING ORGANIZATION Naval Postgraduate School			
6c. ADDRESS (City, State, and ZIP Code) Monterey, CA 93943-5000		7b. ADDRESS (City, State, and ZIP Code) Monterey, CA 93943-5000			
8a. NAME OF FUNDING / SPONSORING ORGANIZATION	8b. OFFICE SYMBOL (If applicable)	9. PROCUREMENT INSTRUMENT IDENTIFICATION NUMBER			
8c. ADDRESS (City, State, and ZIP Code)		10. SOURCE OF FUNDING NUMBERS			
		PROGRAM ELEMENT NO.	PROJECT NO.	TASK NO.	WORK UNIT ACCESSION NO.
11. TITLE (Include Security Classification) COMPUTERIZED MEASUREMENT OF THERMOACOUSTICALLY GENERATED TEMPERATURE GRADIENTS					
12. PERSONAL AUTHOR(S) Kite, Milton David					
13a. TYPE OF REPORT Master's Thesis	13b. TIME COVERED FROM TO	14. DATE OF REPORT (Year, Month, Day) December 1988	15. PAGE COUNT 55		
16. SUPPLEMENTARY NOTATION The views expressed in this thesis are those of the author and do not reflect the official policy or position of the Department of Defense or the U.S. Government					
17. COSATI CODES			18. SUBJECT TERMS (Continue on reverse if necessary and identify by block number)		
FIELD	GROUP	SUB-GROUP	Acoustics, Thermoacoustics, Thermoacoustic Heat Transport,		
			Theses. (mym) ←		
19. ABSTRACT (Continue on reverse if necessary and identify by block number)					
<p>The computerized measurement of thermoacoustically generated temperature gradients in short, thin plates is reported. The computerized data acquisition system is delineated. The temperature difference developed across a stack of short plates was measured as a function of the longitudinal position of the plates in a resonant tube for acoustic pressure amplitudes of 0.5 to 6.6 kPa, and static (or mean) pressure readings of 100 through 440 kPa, in argon and helium for the first through the third harmonic frequencies of the tube. Measured data were compared with predictions based on work done by Wheatley and others [J. Wheatley, et al., Journal of the Acoustical Society of America, v.74, pp. 153-170, 1983] and results reported by Muzzerall (Master's Thesis in Engineering Acoustics, Naval Postgraduate School, Monterey, CA, September 1987). For low acoustic and static pressures, there is good agreement between measured data and theory. As pressures increase there is a general degradation of agreement up to the point at which it appears saturation of the thermoacoustic effect occurs.</p>					
20. DISTRIBUTION/AVAILABILITY OF ABSTRACT <input checked="" type="checkbox"/> UNCLASSIFIED/UNLIMITED <input type="checkbox"/> SAME AS RPT <input type="checkbox"/> DTIC USERS			21. ABSTRACT SECURITY CLASSIFICATION Unclassified		
22a. NAME OF RESPONSIBLE INDIVIDUAL Anthony A. Atchley			22b. TELEPHONE (Include Area Code) (408) 646-2848	22c. OFFICE SYMBOL Code 61Ay	

DD FORM 1473, 84 MAR

83 APR edition may be used until exhausted
All other editions are obsolete

SECURITY CLASSIFICATION OF THIS PAGE

U.S. Government Printing Office: 1986-606-243

UNCLASSIFIED

Approved for public release; distribution is unlimited.

Computerized Measurement of Thermoacoustically Generated
Temperature Gradients

by

Milton David Kite
Lieutenant Commander, United States Navy
B.A., University of Kansas, 1974

Submitted in partial fulfillment of the
requirements for the degree of

MASTER OF SCIENCE IN ENGINEERING ACOUSTICS

from the

NAVAL POSTGRADUATE SCHOOL
December 1988

Author:



Milton David Kite

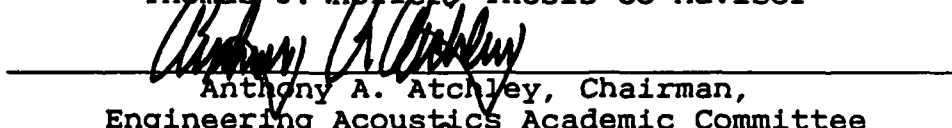
Approved by:



Anthony A. Atchley, Thesis Advisor



Thomas J. Heller, Thesis Co-Advisor



Anthony A. Atchley, Chairman,
Engineering Acoustics Academic Committee



Gordon E. Schacher,
Dean of Science and Engineering

ABSTRACT

The computerized measurement of thermoacoustically generated temperature gradients in short, thin plates is reported. The computerized data acquisition system is delineated. The temperature difference developed across a stack of short plates was measured as a function of the longitudinal position of the plates in a resonant tube for acoustic pressure amplitudes of 0.5 to 6.6 kPa, and static (or mean) pressures from 100 to 440 kPa, in argon and helium for the first through the third harmonic frequencies of the tube. Measured data were compared with predictions based on work done by Wheatley and others [J. Wheatley, et al., Journal of the Acoustical Society of America, v. 74, pp. 153-170, 1983] and results reported by Muzzerall (Master's Thesis in Engineering Acoustics, Naval Postgraduate School, Monterey, CA, September 1987). For low acoustic and static pressures, there is good agreement between measured data and theory. As the acoustic pressure amplitudes increase there is a general degradation of agreement up to the point at which it appears saturation of the thermoacoustic effect occurs.

iii



Accession For	
NTIS GRA&I	<input checked="checked" type="checkbox"/>
DTIC TAB	<input type="checkbox"/>
Unannounced	<input type="checkbox"/>
Justification	
By	
Distribution/	
Availability Codes	
Avail and/or	
Dist	Special
A-1	

TABLE OF CONTENTS

I. INTRODUCTION.....	1
II. THEORY.....	3
A. BASIC THEORY.....	3
B. MUZZERALL'S RESULTS.....	9
III. APPARATUS.....	12
A. TUBE AND PRESSURE VESSEL.....	12
1. Resonant Tube.....	12
2. Pressure Vessel.....	13
3. Driver.....	13
4. Plumbing.....	15
B. TAC.....	15
C. DACQ.....	17
D. LINEAR POSITIONING.....	17
IV. MEASUREMENT.....	21
A. PROCEDURE.....	21
B. RESULTS.....	24
C. DISCUSSION.....	25
V. SUMMARY/RECOMMENDATIONS.....	45
LIST OF REFERENCES.....	46
INITIAL DISTRIBUTION LIST.....	47

ACKNOWLEDGEMENT

First and foremost I would like to thank my thesis advisors, Dr. Anthony Atchley and Dr. Thomas Hofler, without whom, frankly, this thesis would still not be finished. From deciphering "foreign" computer languages to soldering teeny tiny little wires, their assistance was invaluable and greatly appreciated.

Next, George Jaksha and Steve Blankschein of the physics department machine shop deserve a special thanks. Their ability to go from a "big picture" drawing to finished product defies description.

My typist Sherie Gibbons deserves special recognition as well. Turning pages of hand written notes covered with a sea of green ink into a legible form is, in a word, amazing.

I reserve a special thanks for my main support throughout all of my efforts here - my wife Jackie. She who kept me to the straight and narrow and who had the great good sense to be gone whilst I took my data.

Thank you all!

I. INTRODUCTION

The investigation of thermoacoustic heat engines was begun by Wheatley and associates in the early 1980's [References 1 & 2]. They explored the phenomena upon which these engines are based by introducing a thermoacoustic couple (TAC) into an acoustic standing wave. A TAC is a stack of short, thin plates. At least one of those plates is instrumented with a series of thermocouples to measure temperature difference developed across it as a result of the heat transport. In 1987, Muzzerall [Ref. 3] made measurements of the temperature difference developed across a TAC as a function of the position of the TAC in the acoustic field and compared the results to the theoretical value given by Wheatley, et al. There was good agreement between the measured data and the theory at low acoustic pressure amplitude however, at high pressure amplitude there was agreement only in the regions near the pressure antinodes. Elsewhere, unaccountable severe skewing and an overall reduction in the temperature difference was observed.

Muzzerall published extensive data only at two acoustic pressure amplitudes separated by 12 dB. Also, his spatial resolution was only 1 cm. The purpose of the experiment reported in this thesis is to extend this investigation to see where the theory and measured data start to diverge and to further explore

what happens at high acoustic and mean pressures. In order to accomplish these goals, better spatial resolution and the ability to investigate a broader range of parameters is required. The parameters to be controlled are acoustic pressure amplitude, ambient (or mean) pressure, frequency, and gas type. In order to handle the quantity of data recorded and to ensure repeatability of measurements, both the data acquisition and the linear positioning of the TAC are computer controlled in this investigation. Following a derivation of the theoretical basis for the generation of temperature gradients and a summary of Muzzerall's results, the computer controlled experimental apparatus is delineated. Methodology for data acquisition is discussed and a graphical comparison of measured and theoretical data is made. Areas for further investigation are included.

II. THEORY

Wheatley, et al. [Ref. 2] used the term "natural engine" to describe a process where a phase shift is introduced between temperature and velocity by a natural, irreversible process - here thermal conduction. This process leads to, what has been termed, thermoacoustic heat transport. The TAC acts as such an engine establishing a thermal lag which drives an entropy flow. A brief description of this phenomena is described below. A detailed development of theoretical thermoacoustics applied to engines is given by Swift [Ref. 4].

Following the description of the phenomenon, a summary of Muzzerall's findings is presented.

A. BASIC THEORY

The cyclic heat pumping action of the TAC as a "natural engine" may best be described from a Lagrangian point of view. Referring to Figure 1, a poor thermally conducting plate is located near the end of a rigid resonant tube. A sound source is located at the left end of the tube (not shown). This source generates an acoustic standing wave in the tube. Consider a parcel of gas located near (within a thermal penetration depth) the plate. Both the plate and the parcel of gas are initially at

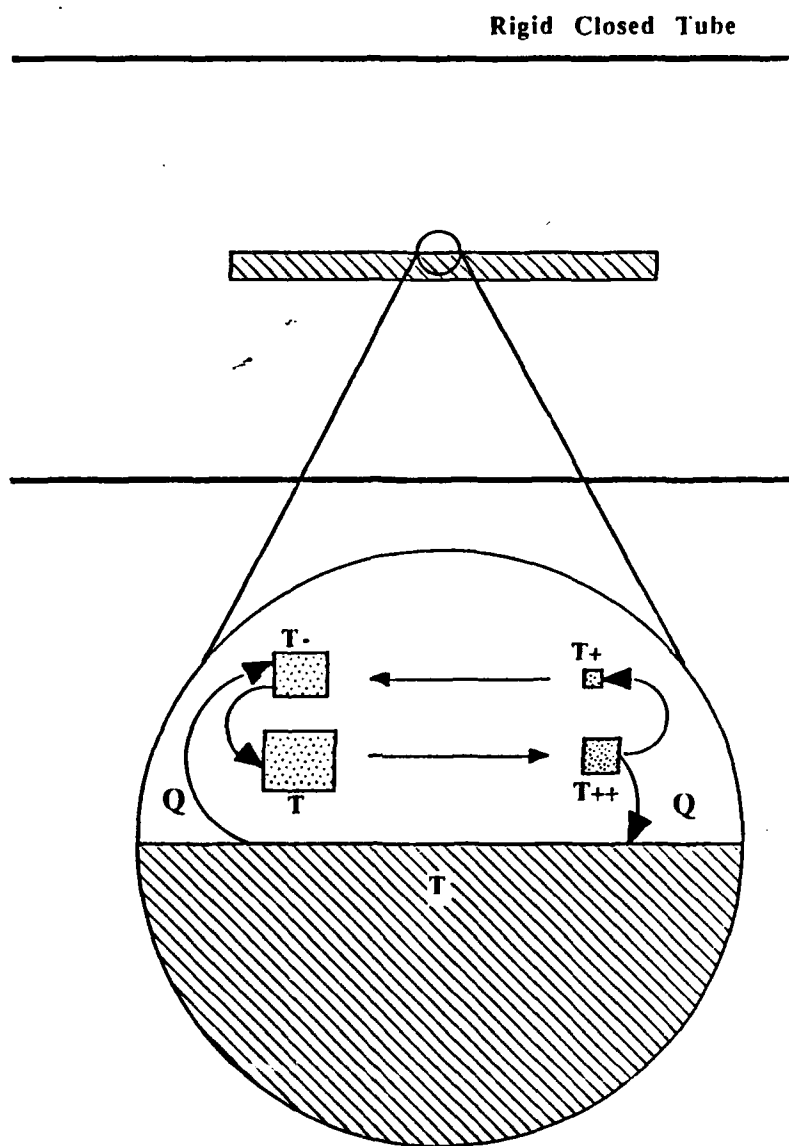


Figure 1
The Thermoacoustic Effect

temperature T . During the compression phase of the acoustic cycle the parcel is displaced toward the pressure antinode and undergoes an adiabatic compression increasing its temperature to $T++$. The temperature difference drives a heat flow (Q) from the gas to the plate reducing the parcel's temperature to $T+$. On the expansion phase of the acoustic cycle, the gas undergoes an adiabatic expansion, but is now at the lower temperature $T-$. Here the temperature difference results in a heat flow in the opposite direction, returning the gas parcel to its original temperature T . The result is that after one cycle, the parcel has transported an amount of heat Q over a short distance. The deposited heat is picked up by an adjacent parcel and moved still further during the next cycle. The heat is shuttled down the plate, toward the closed end of the tube, until it reaches the end of the plate. There it collects, until conducted back through the plate or the surrounding gas.

The system reaches steady state when the hydrodynamic heat (entropy) flow in the gas is balanced by the return diffusive heat (entropy) flow in the plate and in the surrounding gas. The entropy flow increases when there is no average temperature gradient in the plate. As the gradient increases, the heat flow begins to drop. There exists a critical gradient beyond which acoustics alone will no longer increase the temperature gradient in the plate [Ref. 1]. The gradients from zero through the

critical value demark the heat pump regime, which is addressed specifically in this thesis.

The behavior of the temperature difference as a function of its position in the standing wave can be derived from Wheatley's estimate for the time-average hydrodynamic heat flow [Ref. 1: p. 156, Eqn. 15]:

$$\dot{Q} \approx \pi \delta_k (T_m \beta) (\Gamma - 1) p_1 u_1$$

where

π = overall perimeter of the plate

δ_k = thermal penetration depth

T_m = mean temperature

β = isobaric expansion coefficient

p_1 = acoustic pressure magnitude

u_1 = acoustic velocity magnitude

Γ = defined by Wheatley as the ratio of $\nabla_T / \nabla_{T_{crit}}$

The terms $T_m \beta$ determine the adiabatic temperature change per pressure change and $\pi \delta_k$ is the volume of gas-plate interaction. $(\Gamma - 1)$ shows how the entropy flow changes as the temperature gradient changes and becomes zero at $\nabla_T = \nabla_{T_{crit}}$. The next step in the development [Ref. 1: p. 158, Eqn. 30] is to note that:

$$\Delta T = \langle \dot{Q}_2 \rangle / (kA/l)$$

where

k = thermal conductivity

A = sectional area of the plate

l = effective length of couple

$\langle \dot{Q}_2 \rangle$ = spatial average with subscript 2 denoting second order validity

The relationship between acoustic pressure, velocity and the temperature difference is seen in Figure 2 for arbitrary units.

Wheatley's expression for the temperature difference across the TAC [Ref. 2: p. 157, Eqn. 17] is:

$$\Delta T = \frac{\frac{P_o^2 \delta_k (1 + \sqrt{\sigma}) \sin(2KX)}{4 \rho_o a \left(\frac{K_p d_p}{1} + \frac{K_g d_g}{1} \right) (1 + \sigma)}}{1 + \left[\frac{P_o^2 \delta_k (1 - \sigma^{3/2})}{4 \left(\frac{K_p d_p}{1} + \frac{K_g d_g}{1} \right) \rho_o l T_m (\sigma - 1)(1 - \sigma^2)} \right] [1 - \cos 2KX]}$$

with

$$\Delta T = T_{cold} - T_{hot}$$

P_o = acoustic pressure (AC pressure)

σ = Prandtl #

δ_k = thermal penetration depth

a = sound speed

K = wave number

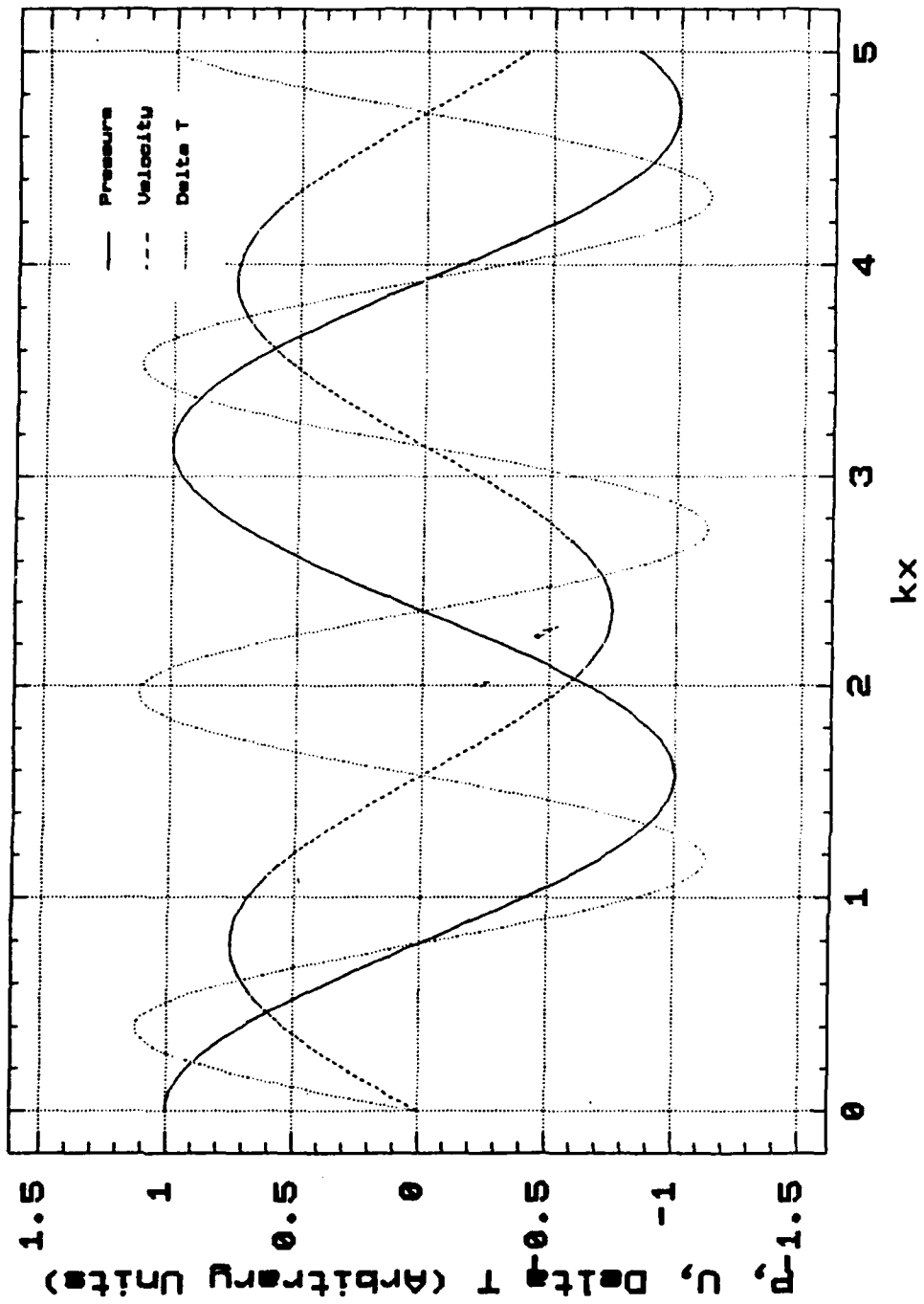


Figure 2
Spatial Dependence of Pressure, Velocity and T

x = distance from closed end of tube

ρ_o = mean density

k_p, k_g = thermal conductivity for plate(p) and gas(g)

l = length of TAC

T_m = TAC temperature

$\omega = 2\pi$. frequency

γ = ratio of specific heats, C_p/C_v

which is what was used to determine the theoretical values in this paper.

B. MUZZERALL'S RESULTS

Included for comparison are Muzzerall's results (Figures 3 and 4) for a TAC made of stainless steel plates 2.26 cm long x 2.16 cm wide, at four penetration depth spacing. These measurements were made in argon at a frequency of 705Hz and a static pressure of one atmosphere. The lines indicated as theory are the predictions of the expression given previously for ΔT . The acoustic pressure amplitude in Figure 3 is 630 kPa. There is overall good agreement between theory and experiment. In Figure 4 the acoustic pressure amplitude has been increased to 2500 kPa. The overall agreement between theory and experiment is severely diminished, although it is still quite good in regions near acoustic velocity nodes. The impetus behind the present thesis is to explore the regions between and beyond these two figures in order to better understand the reasons for this behavior.

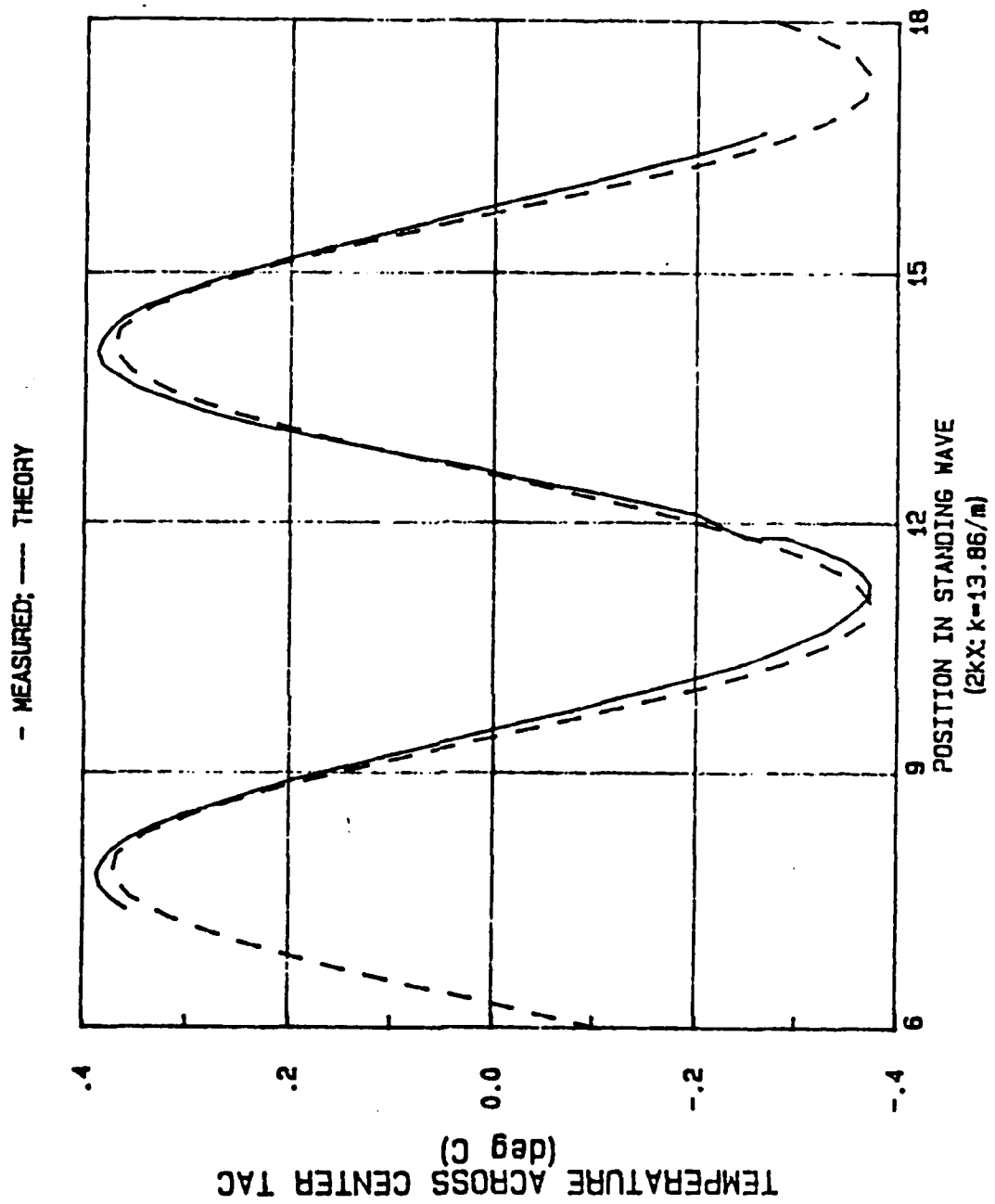


Figure 3
Muzzerall's Results 150dB

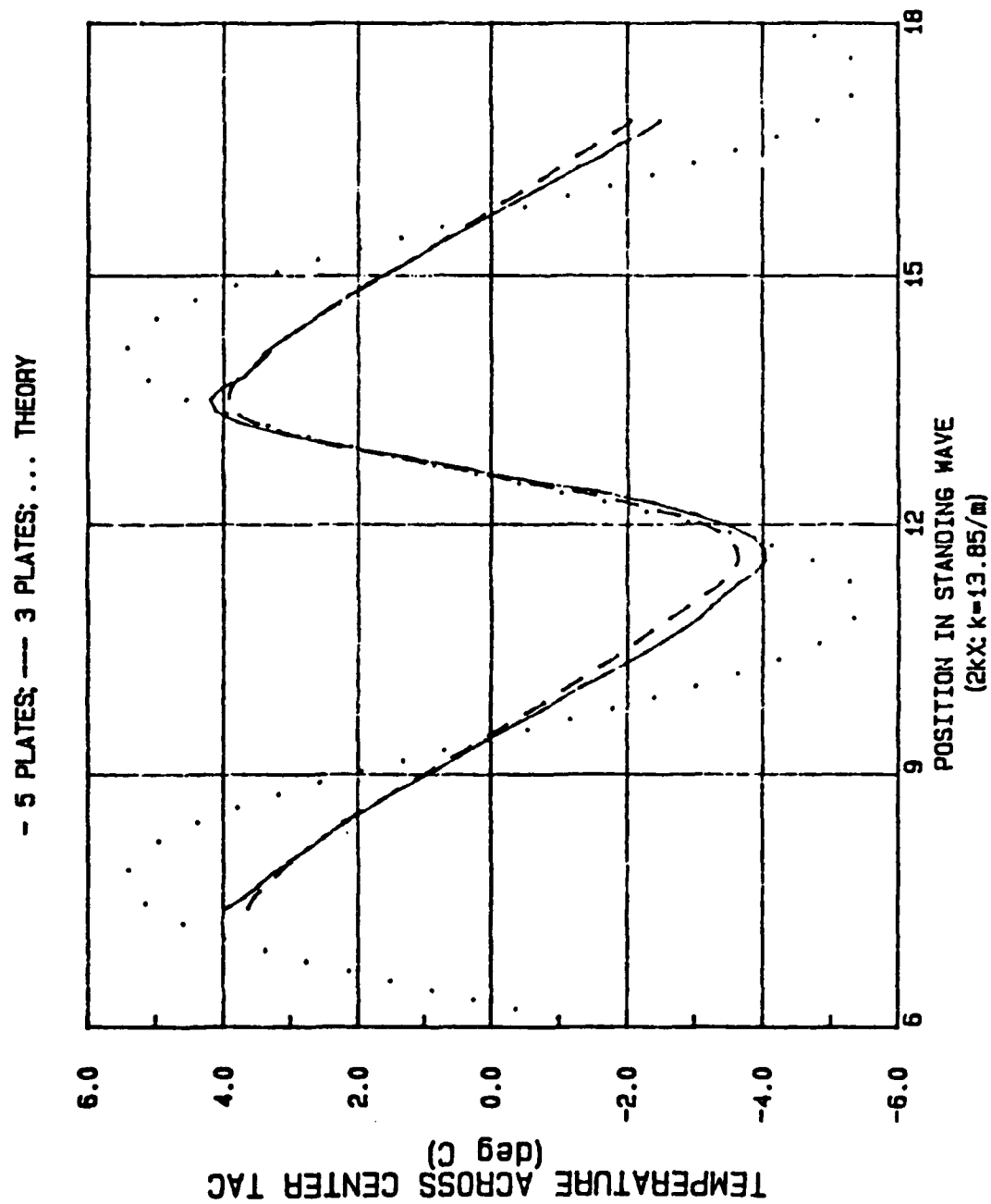


Figure 4
Muzzerall's Results 162dB

III. APPARATUS

The experimental apparatus can most easily be described by breaking it down into its functional component parts. The subsystems are: the tube and pressure vessel, the TAC; the linear positioning system; and the data acquisition (DACQ) system. A brief description of the function of these subsystems is given along with block diagrams for each.

A. TUBE AND PRESSURE VESSEL

1. Resonant Tube

The tube is a 1.22 m long, 3.81 cm inside diameter copper tube. The length was chosen to obtain one half of an acoustic wavelength - therefore a full thermal wavelength - at the fundamental. The tube is soft soldered to brass flanges which are attached to the pressure vessel at one end and a blanking plate at the other. The purpose of the blanking plate is to provide a rigid termination. An Endevco model 8510B-5 piezoresistive transducer is threaded through the blanking plate and used to measure the acoustic pressure. A 1/8" diameter stainless steel probe tube, which carries the TAC, also goes through the blanking plate. It is supported in the center of the plate by a rubber O-ring compression fitting. In order to allow

for elevated mean pressures within the tube, the volume behind the Endevco piezoresistive diaphragm is connected to the resonant tube via a capillary leak, which allows pressure equalization, but blocks acoustic pressure oscillations. The tube is wrapped with insulation material to ensure thermal isolation. (Figure 5).

2. Pressure Vessel

The ability to increase mean pressure required the acoustic driver (discussed below) to be enclosed in a pressure vessel. The vessel is made out of an aluminum cylinder joined to two aluminum end plates by threaded rods. The cylinder is 30.5 cm long with a 25.4 cm inside diameter and 2.54 cm wall thickness. The end plates are 2.54 cm thick disks, 35.6 cm in diameter. The mean pressure inside the pressure vessel is sensed both by a dial pressure gauge and by an OMEGA Model PX304-150AV pressure transducer mounted in the back end plate. A 150 psi relief valve is mounted on the pressure vessel end plate.

3. Driver

The acoustic driver is a JBL Model 2445J compression driver with input provided by a Hewlett Packard Model 3314A Function Generator amplified by a Techron Model 7520 Power Supply Amplifier. The driver is mounted on the inside of the pressure

vessel end plate attached to the resonant tube. Provisions are made to enable mounting a positive displacement piston driver for work at high ambient pressures, though it was not used in this experiment.

4. Plumbing

Connections were made to pressurize the tube and pressure vessel, with provisions to equalize the pressure on both sides of the acoustic driver. Connections were also made to attach a vacuum pump, with a needle valve for controlled backfilling, and also a system vent for outlet.

B. TAC

The TAC is a stack of 6 G-10 fiberglass plates, 1 cm long by 2.54 cm wide (Figure 6). The center two plates are glued together with four type E (chromel-constantan) thermocouples in between. The thermocouples are connected in series to increase the output voltage and they allow the measurement of temperature difference across the TAC. The spacing between the center "sandwich" and the remaining guard plates is 1.54 mm. A thermocouple is glued to the back edge of one of the guard plates, which allowed the measurement of the absolute TAC temperature. The center plate sandwich is 0.595 mm thick and the guard plates are 0.36 mm thick.

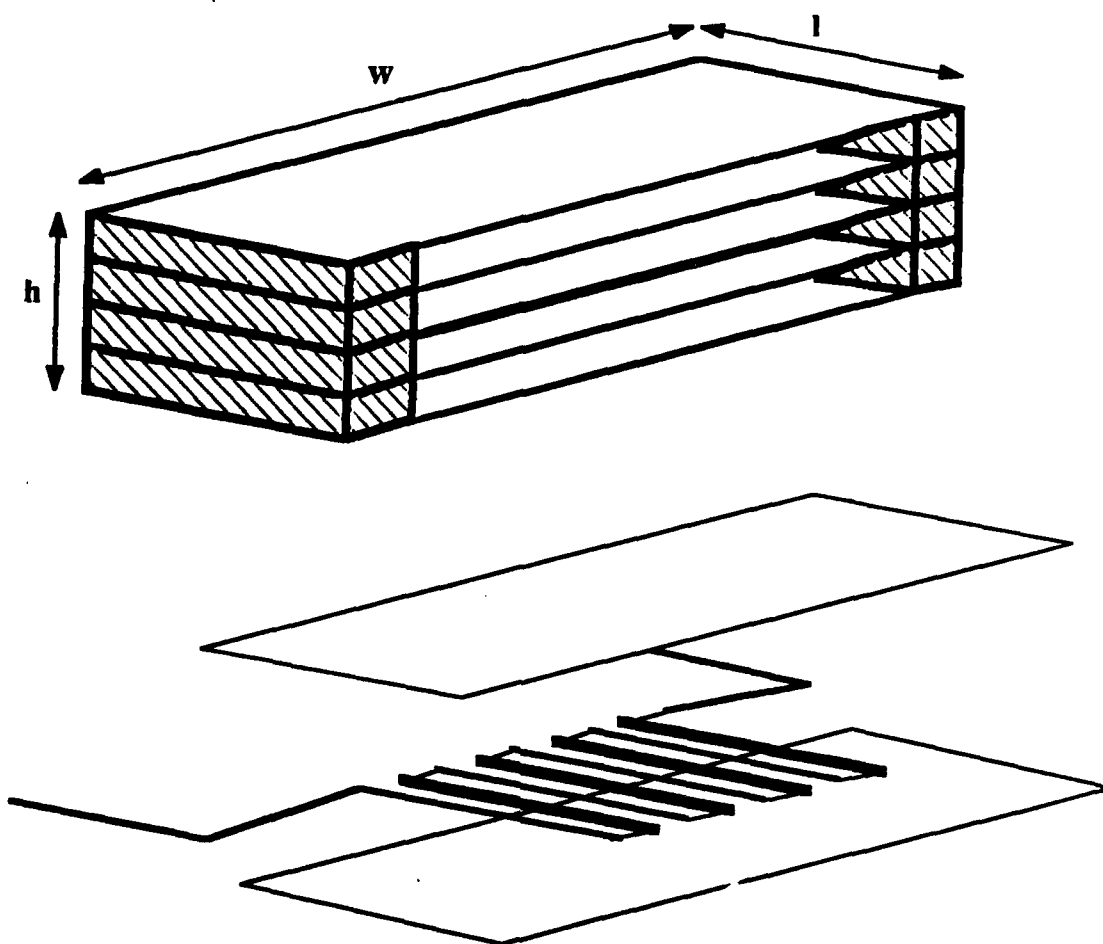


Figure 6
Thermoacoustic Couple (TAC)

C. DACQ

Data acquisition is centered around the HP 3457A multimeter (Figure 5). To reduce the number of connection lines in the figure, circled numbers represent connections to multimeter input channels and the circled "f" the front panel input. The Kikusui Model 6100 Oscilloscope was used to monitor system performance.

The system reference temperature was read from a thermistor which was placed inside an aluminum block to ensure thermal stability (Figure 7). Junctions for tube and TAC temperature thermocouple wires are attached to this block, insuring the chromel-copper and constantan-copper junctions are isothermal.

D. LINEAR POSITIONING

Motive force for TAC positioning is provided by a Compumotor Model M83-135 Stepper Motor (25,000 steps/rev) (Figure 8) which is coupled to a Warner Electric 0.125 Lead Screw (8 turns/inch) on which rides a precision ball nut having zero lash. The ball nut is attached to an arm which slides on a support rod for stability. The other end of the arm is attached to the stainless steel probe tube which holds the TAC. A Compumotor Model 2100 Indexer serves as the interface between a Standard 286 (AT clone) computer and the motor.

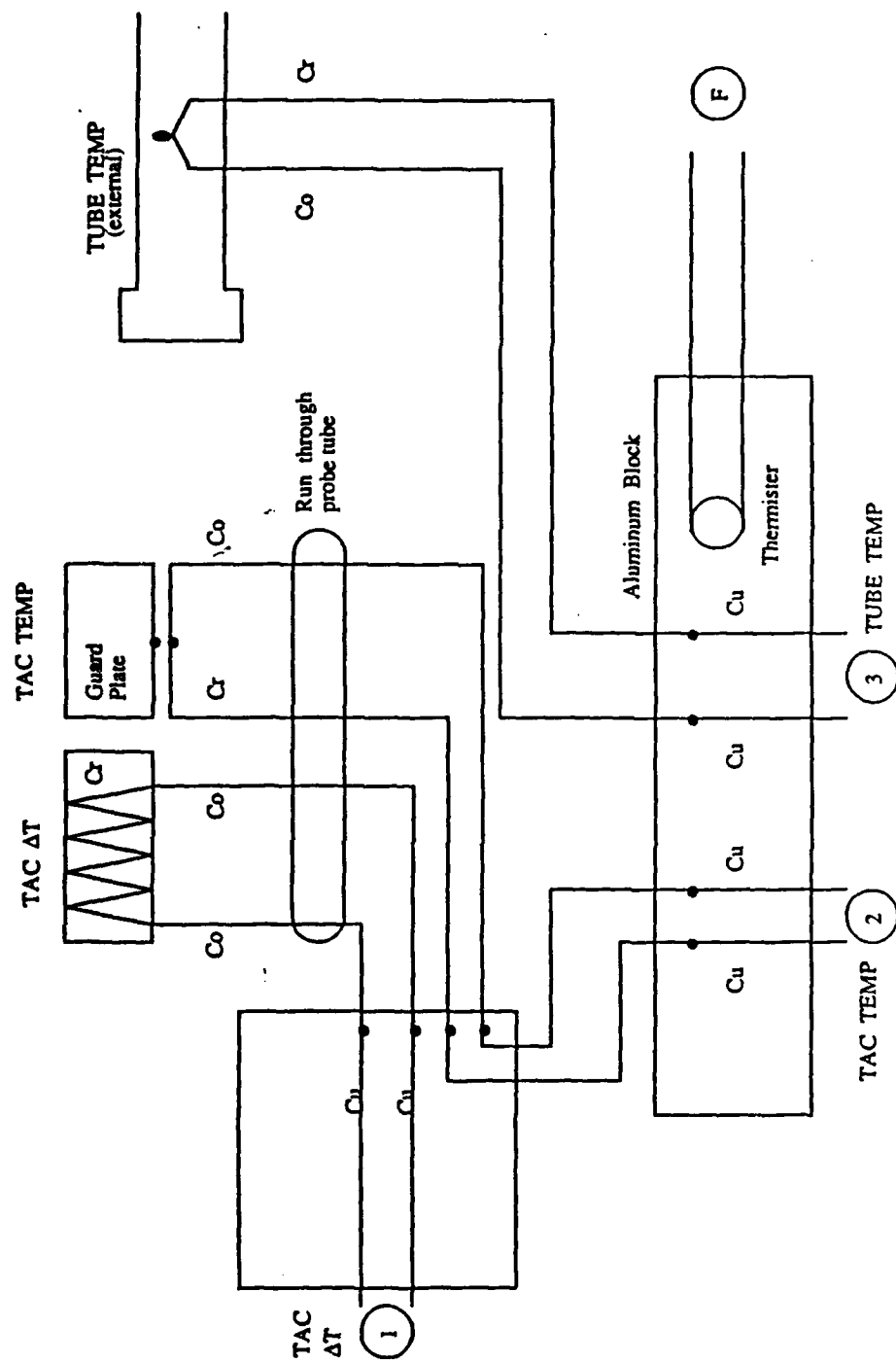


Figure 7
Temperature Reference

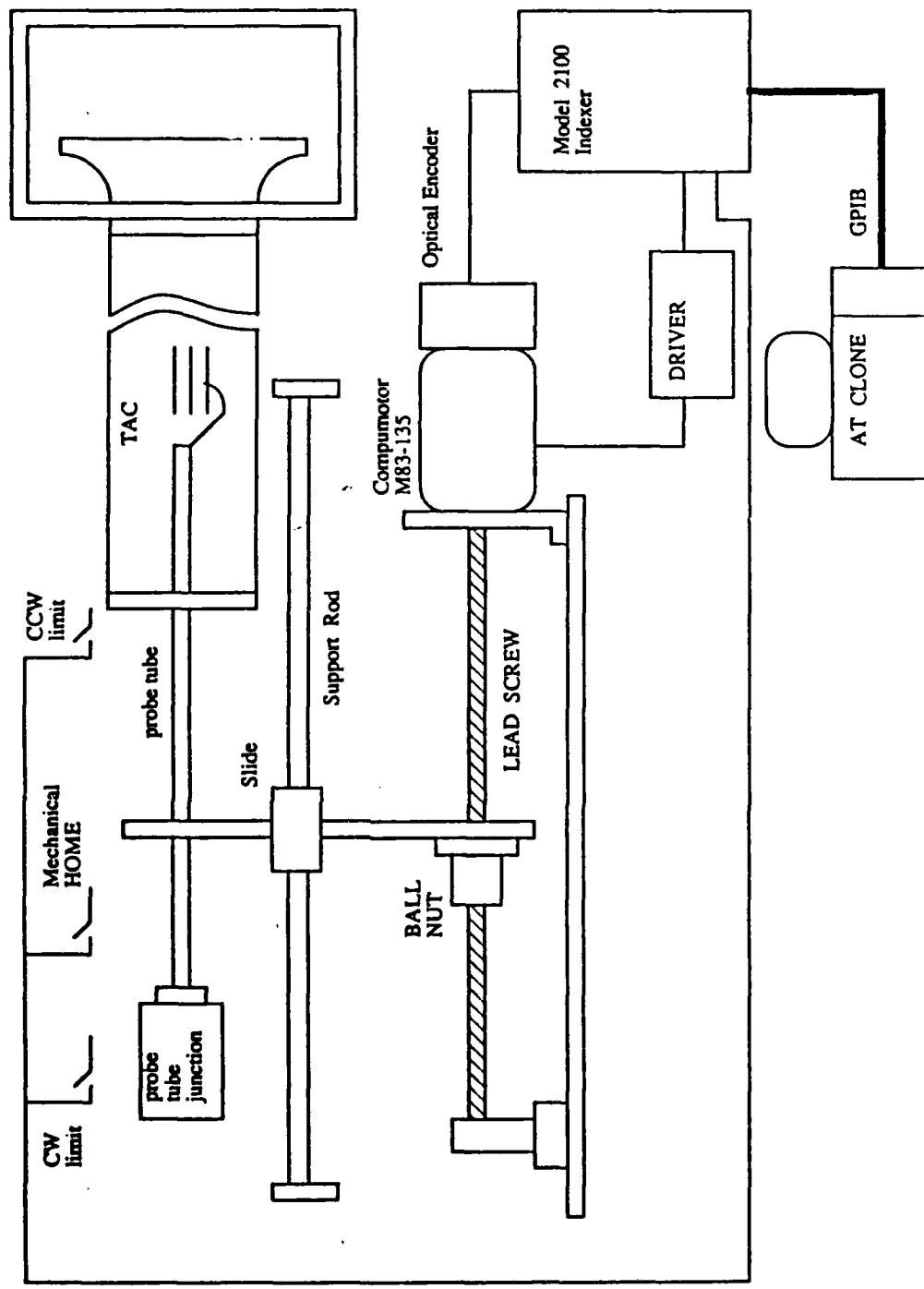


Figure 8
Linear Positioning System

End of travel limit for both CW and CCW rotation and mechanical HOME (or reference) limit switches were tied directly to the indexer. All data runs start from the HOME position. To more precisely define HOME, a 1000:1 optical encoder is used in conjunction with the mechanical home limit switch. Once the mechanical switch activates, rotation is continued until the appropriate index on the encoder wheel is found. Positional repeatability was consistently within 1 motor step, or approximately 0.127 microns of longitudinal travel, assuming the mechanical switch was consistent enough to bring the optical encoder into the proper range.

Interface between the personal computer (PC), the indexer, and the other HP equipment is accomplished through a National Instruments IEEE 488 General Purpose Interface Bus (GPIB) card in the PC.

IV. MEASUREMENT

Development and testing of the experimental apparatus with its complex control and data collection program was a major time consuming undertaking. However the result is that once the system is manually pressurized, all subsequent operations are fully automated.

Data acquisition is highly flexible. For example, the ability to adjust linear positioning step size ensured a data density sufficient to show the most detailed features of the temperature profile. Experimental results are presented in a serial manner with one feature changing per series. A summary figure leads to the discussion section.

A. PROCEDURE

Before data acquisition is started, the system is pumped down and backfilled with either helium or argon several times. Approximate resonance frequencies are determined next by driving the JBL with the noise source of the Signal Analyzer. The Endevco output is then fed back into the Signal Analyzer. The displayed signal peaks denote resonance frequencies. The driver input device is now changed to the function generator which is set to individual resonance frequencies to check for interference

between those resonances and higher harmonics of the drive signal (Figure 9). In general the harmonics were 18 or more dB below the fundamental.

The gain on the voltage amplifier was set to a mid-range position and then left in that position for the duration of the data run. Determination of the magnitude of the amplification was unnecessary as acoustic pressure was measured directly.

Automated data acquisition now begins. The program initially takes voltages from the ambient pressure transducer and directly converts them to pressure. The reference temperature is then read directly from the multimeter and converted to a effective reference voltage through a polynomial. The low order polynomial was numerically determined from NBS thermocouple tables over the limited temperature range of interest. Voltages from both the tube and TAC temperature thermocouples are read, added to the effective reference voltage, and converted to temperatures by an inverse polynomial. The drive voltage amplitude is set on the function generator and a search is made for resonance frequency by stepping on both sides of the previously determined natural frequency and reading the resultant acoustic pressure amplitude. The frequency producing the highest acoustic pressure amplitude is selected and set in the function generator.

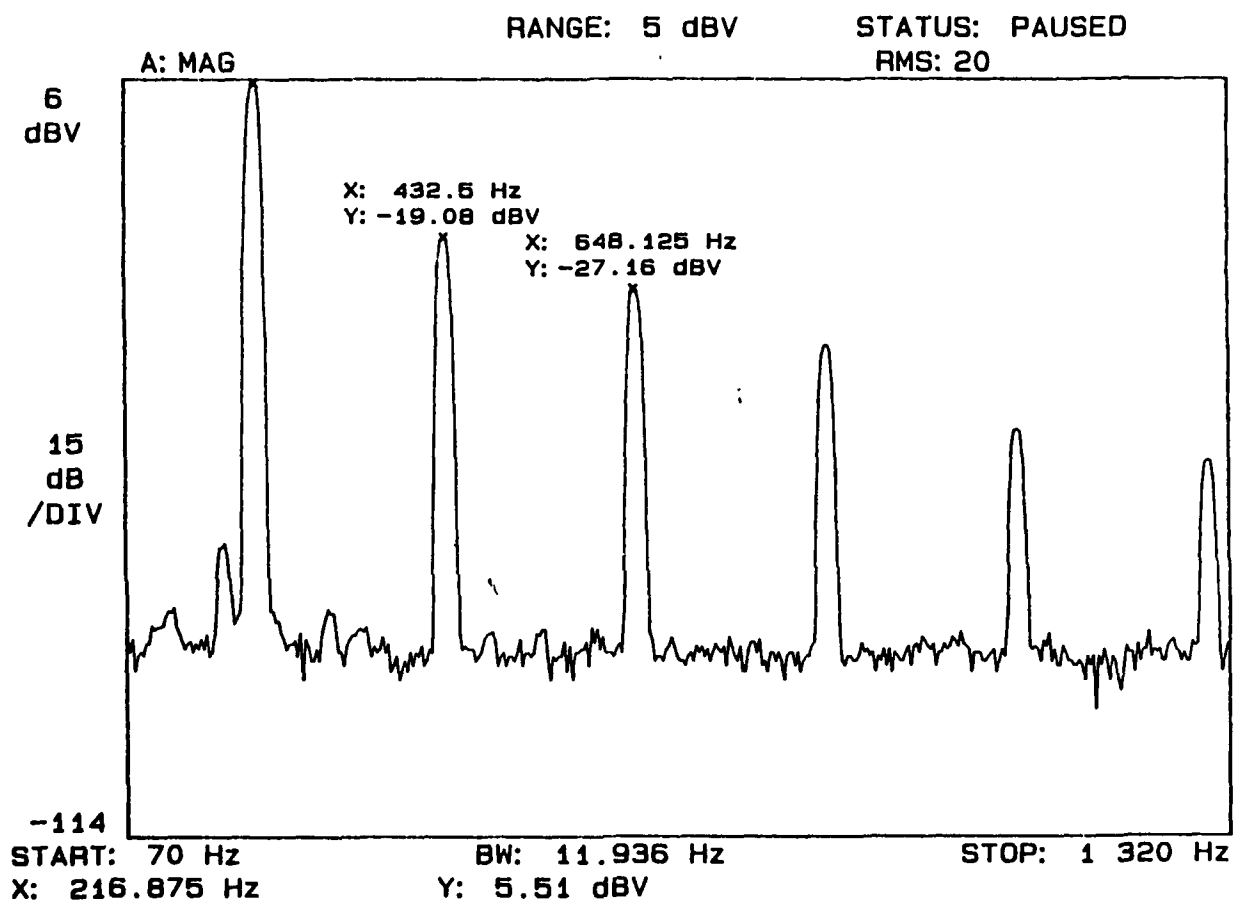


Figure 9
Drive Signal Spectrum

Once the preliminary readings are finished and the function generator set, the data run commences by reading the TAC thermocouple voltage and converting it to a temperature as discussed above. Then the TAC thermopile voltage is read and converted to a temperature differences as follows:

$$\Delta T = \frac{\Delta V}{4} \left[\frac{dT \text{ (type E)}}{dV} \right]_{TAC \ T}$$

ΔT = TAC delta temp

ΔV = TAC thermopile V

dV = TAC thermocouple voltage

dT = TAC temperature

The TAC is then moved to the next position, a wait time, obtained from Muzzerall [Ref. 3], activated and then readings are taken. Multiple data runs were made at constant static pressure and increasing acoustic pressure by resetting the indexer to the home position and incrementing the drive voltage on the function generator.

B. RESULTS

Experimental results are presented here in several series interspersed with theoretical predictions. The ordinate on all of the figures is the temperature differences ($T_H - T_C$) in degrees Kelvin across the TAC. The abscissa is the product of the wave number and the distance of the center of the TAC from the rigid end of the resonance tube. All pressures, acoustic and

ambient are in kilopascals. The first plot (Figure 10) is the only one to show individual data points - all other data is shown by connecting lines. The purpose of this figure is to show the density of data points, which is similar for all the subsequent figures.

The first series (Figures 11, 12, and 13) demonstrate the typical degradation of experimental results against theoretical prediction at increasing acoustic pressures. The next series (Figures 14 through 17) show the effect of shifting from the first through the third overtone. Remaining at the third overtone, the next series (Figures 17 through 21) show increasing ambient pressure in one atmosphere steps. The last series (Figures 22 through 26) shifts to Helium at one atmosphere and shows again increasing frequencies.

C. DISCUSSION

The graphical presentation of the "raw" experimental results show no sharp demarcation between agreement of theoretical prediction and measured data, but demonstrate a gradual degradation of agreement at increasing frequencies and pressures. Several interesting features can be seen in the series.

The first series demonstrate results akin those of Muzzerall [Ref. 3]. Specifically shown is good agreement at velocity nodes

ARGON 415 Hz 1.328 kPa 330 kPa

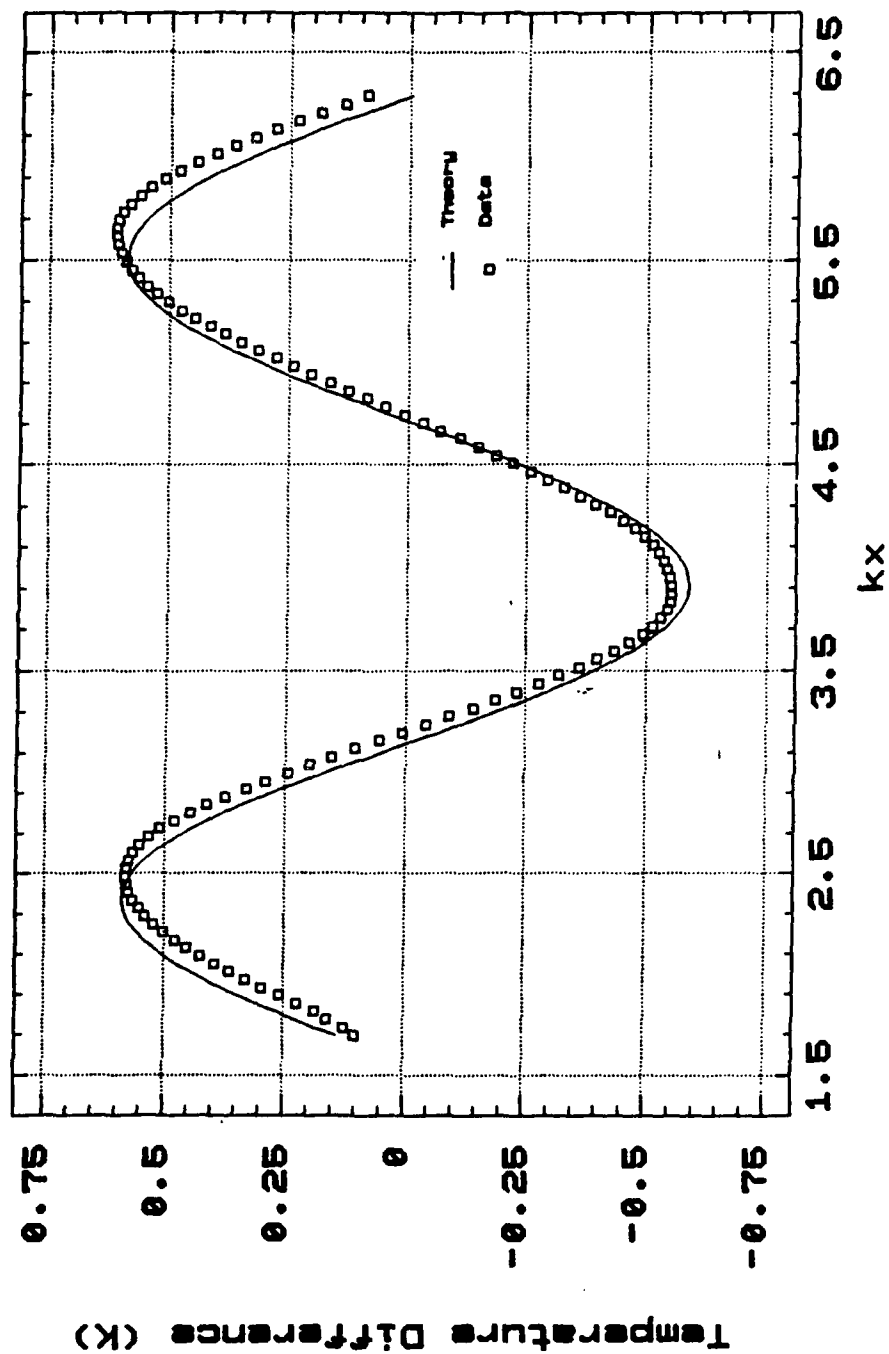


Figure 10
Individual Data Points Plotted

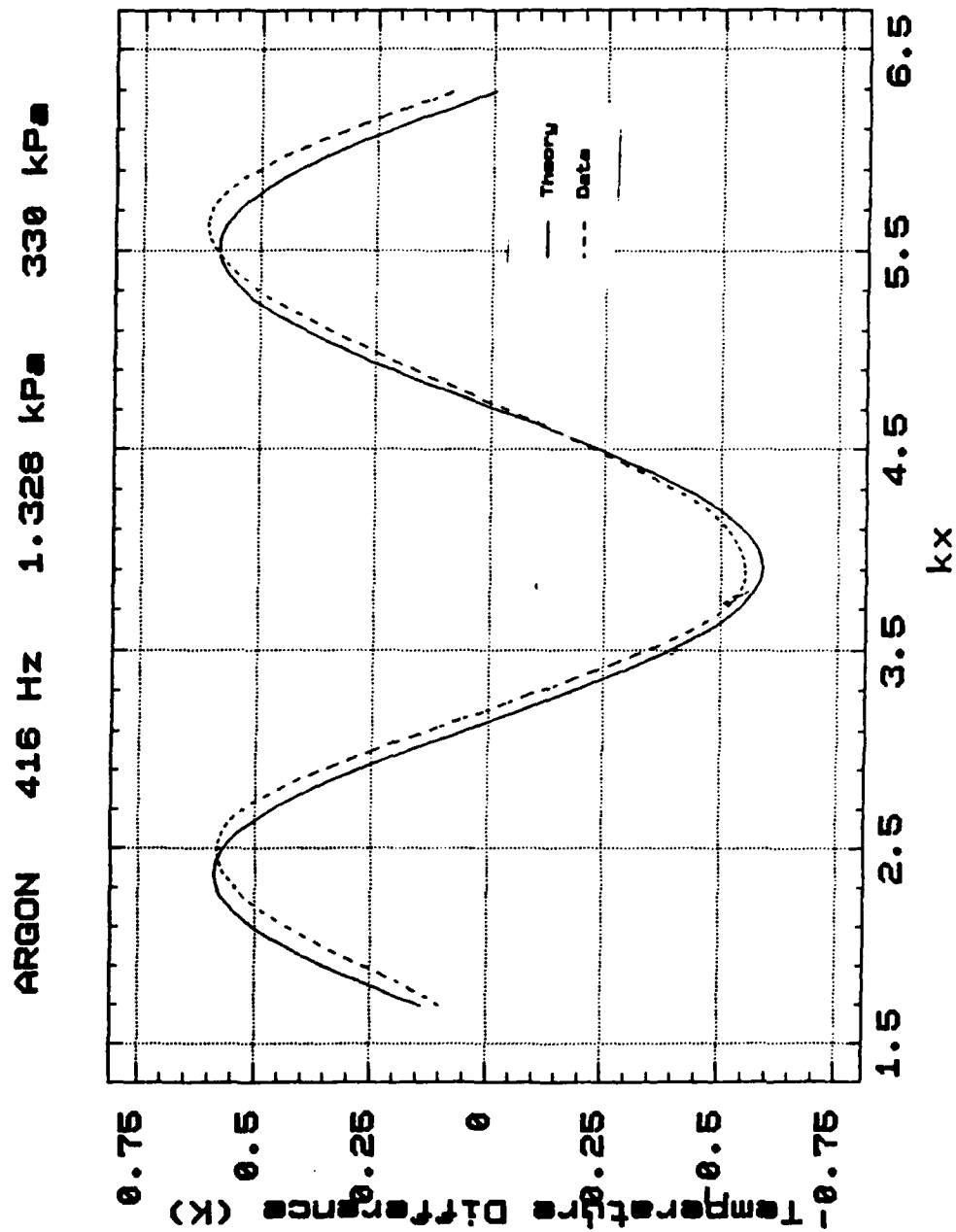


Figure 11
Series 1a Increasing Acoustic Pressure

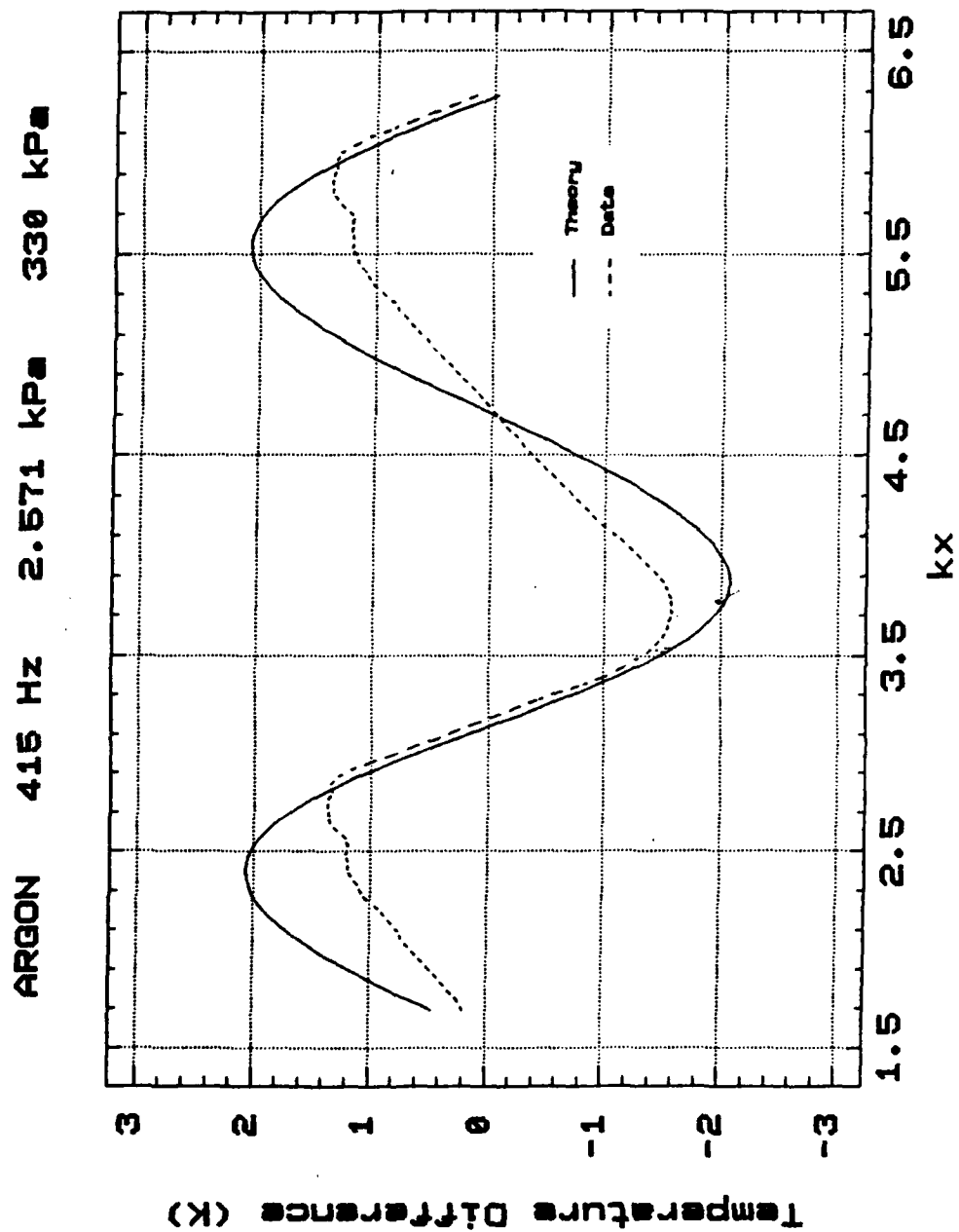


Figure 12
Series 1b Increasing Acoustic Pressure

ARGON 415 Hz 3.184 kPa 330 kPa

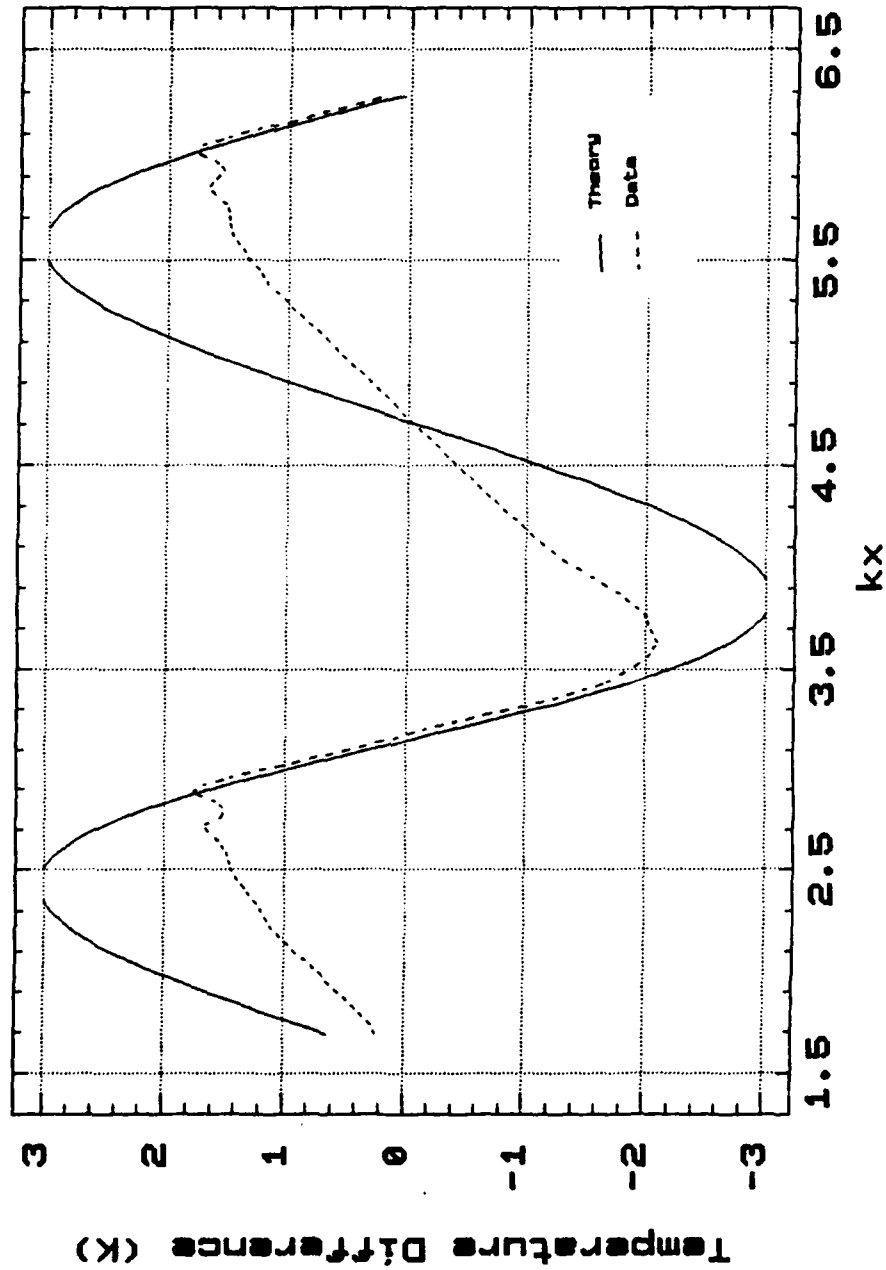


Figure 13
Series 1c Increasing Acoustic Pressure

ARGON THEORETICAL 217 Hz 103 kPa

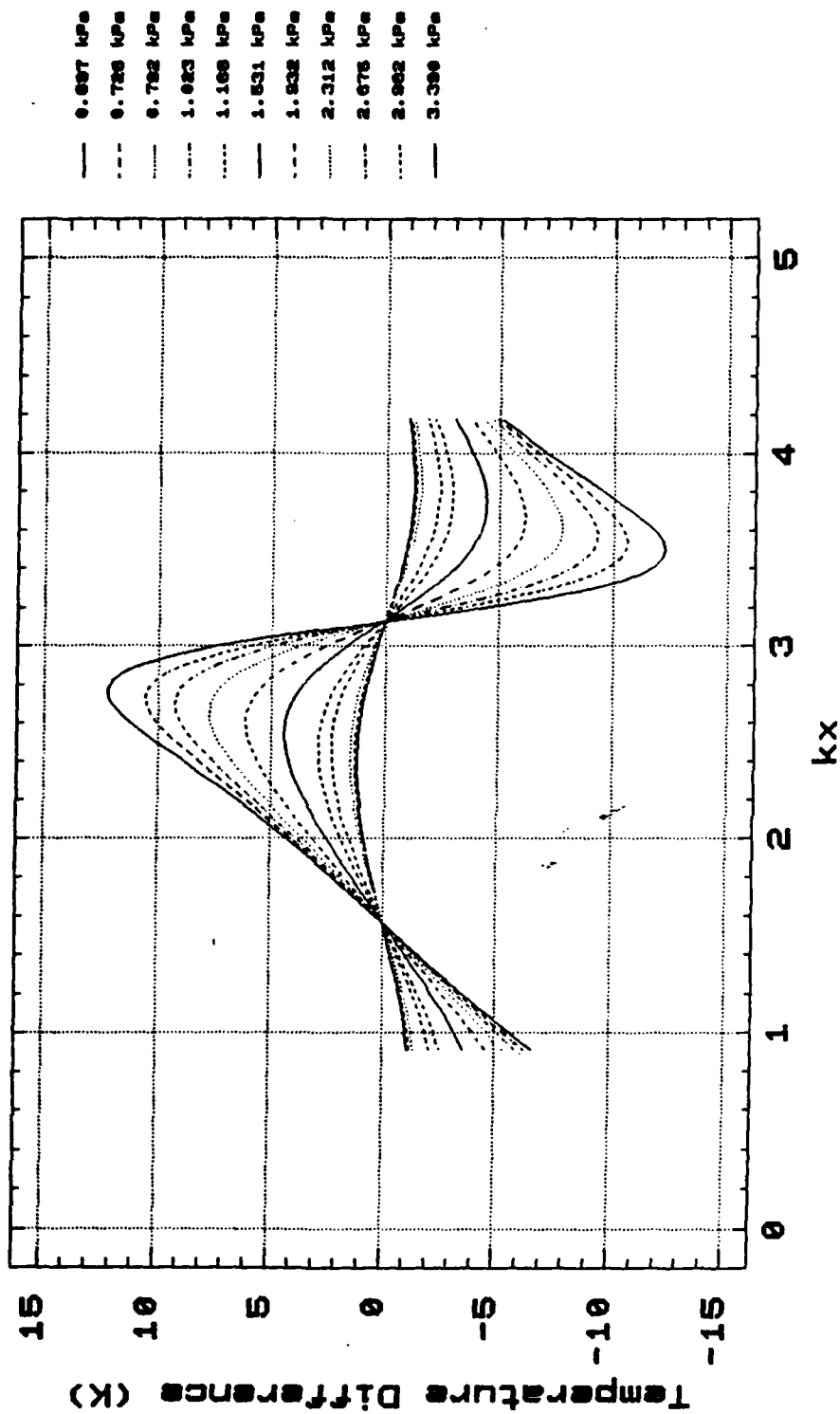


Figure 14
Series 2a Increasing Frequency

ARGON EXPERIMENTAL 217 Hz 103 kPa

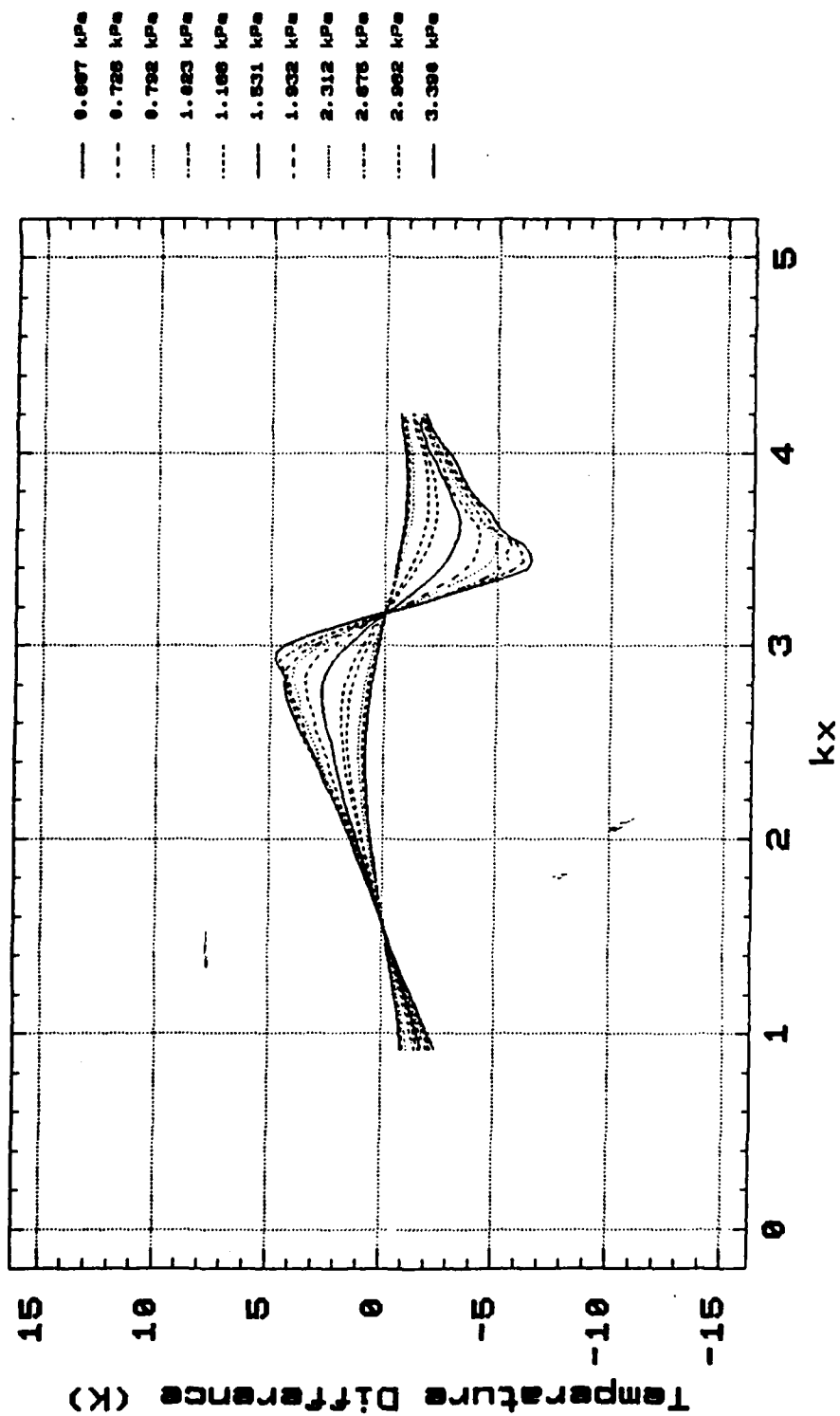


Figure 15
Series 2b Increasing Frequency

ARGON EXPERIMENTAL 331 Hz 103 kPa

Temperature Difference (K)

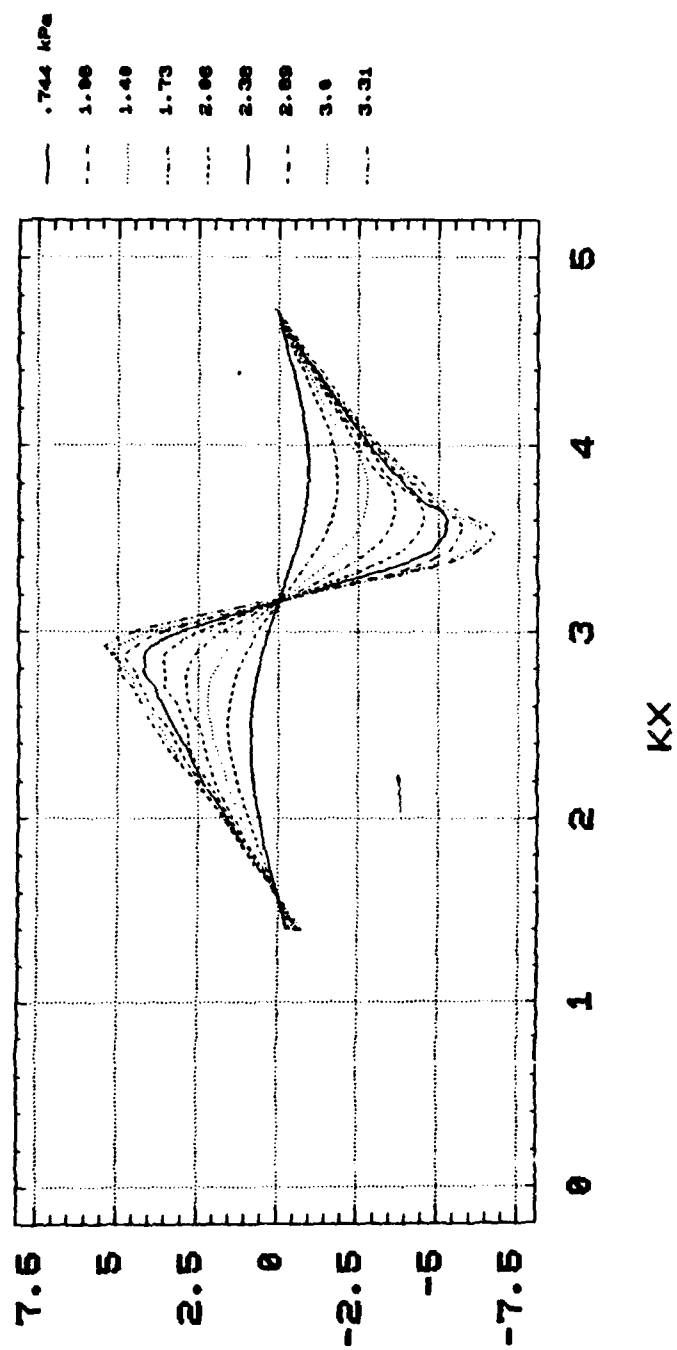


Figure 16
Series 2c Increasing Frequency

ARGON EXPERIMENTAL 449 Hz 103 kPa

Temperature Difference (K)

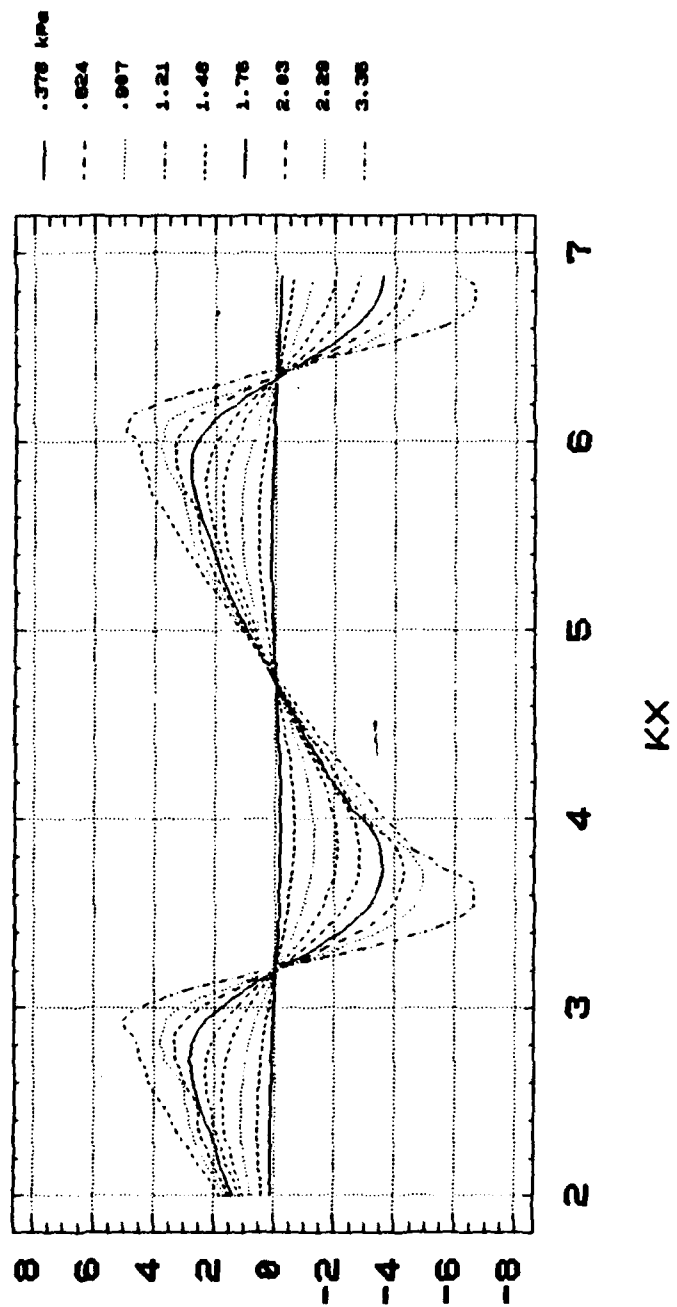


Figure 17
Series 2d Increasing Frequency

ARGON EXPERIMENTAL 426 Hz 200 kPa

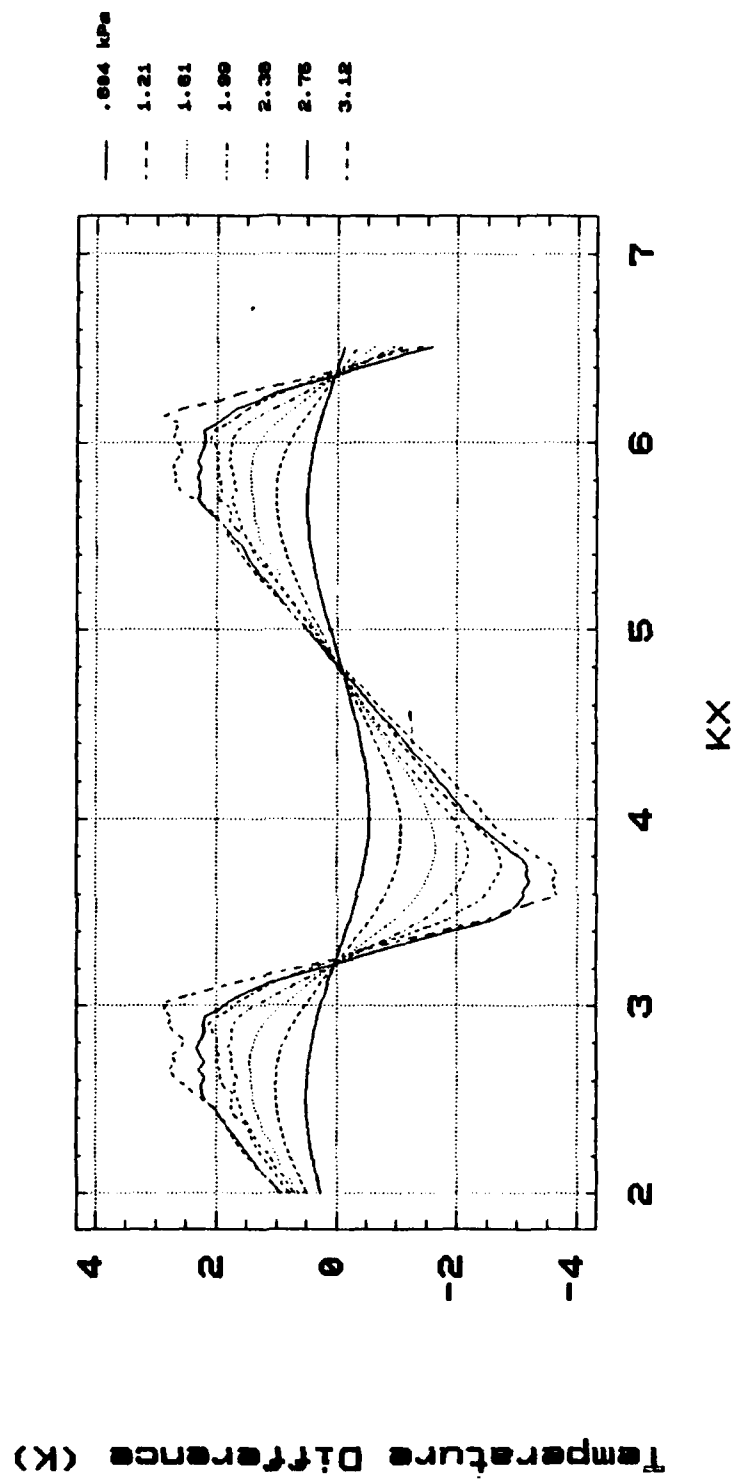


Figure 18
Series 3a Increasing Static Pressure

ARGON THEORETICAL 415 Hz 330 kPa

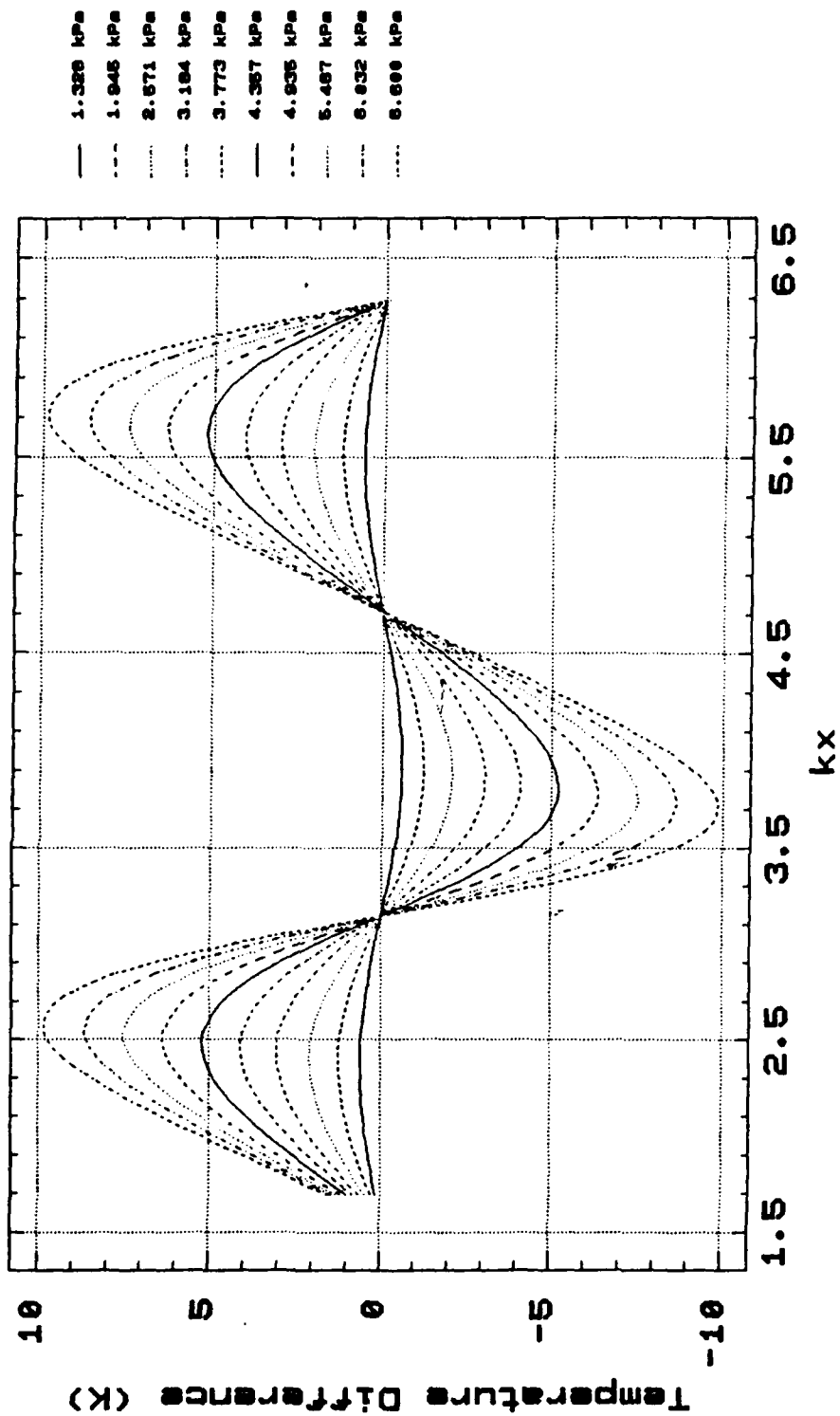


Figure 19
Series 3b Increasing Static Pressure

ARGON EXPERIMENTAL 415 HZ 330 kPa

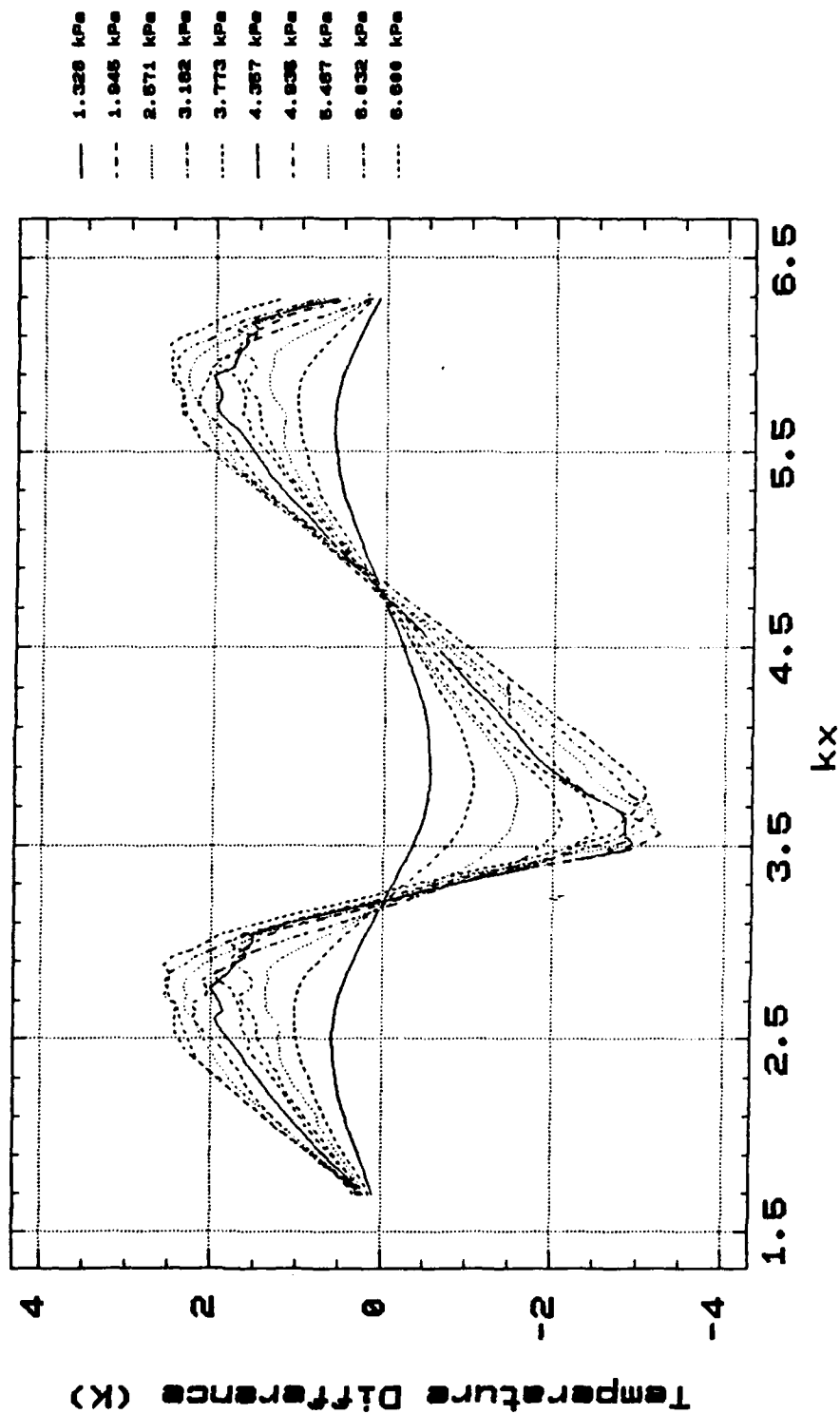


Figure 20
Series 3c Increasing Static Pressure

ARGON EXPERIMENTAL 413 Hz 440 kPa

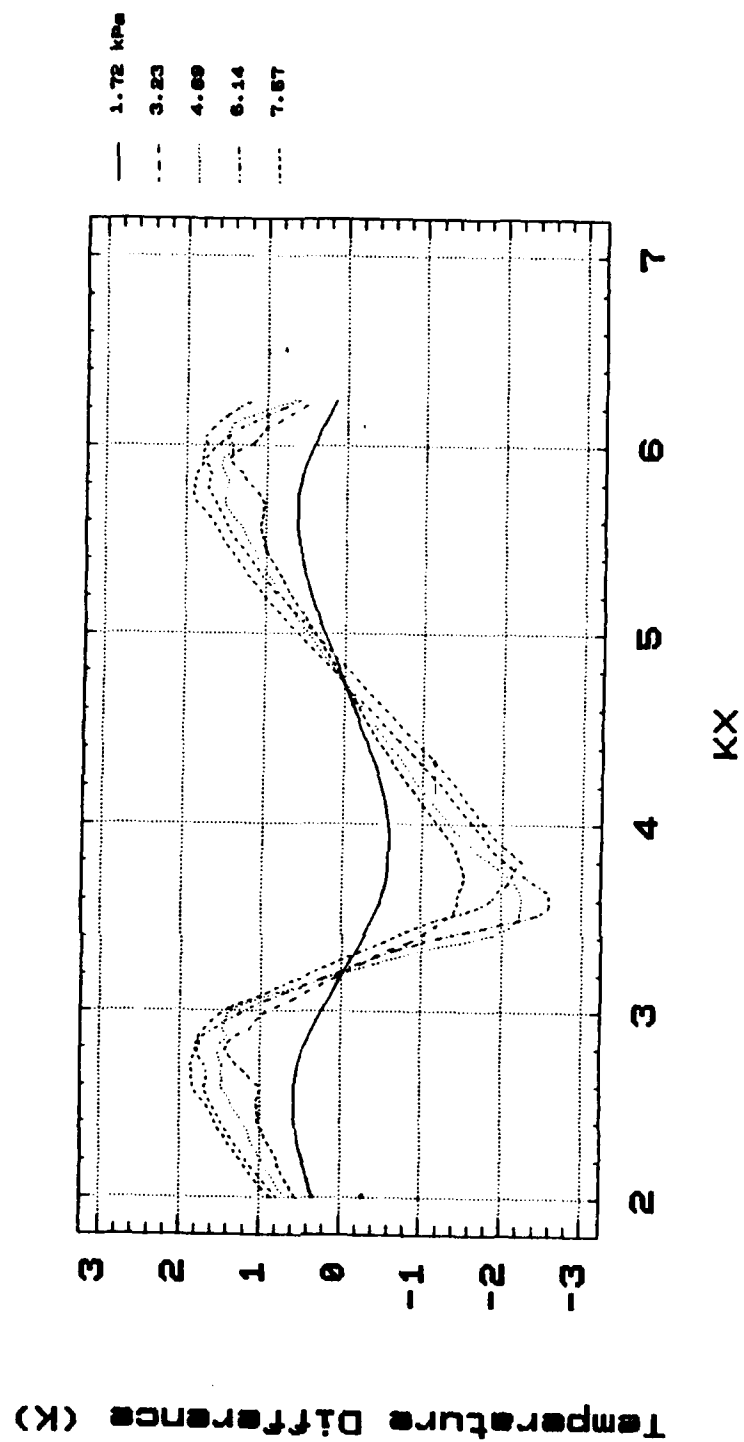


Figure 21
Series 3d Increasing Static Pressure

HELIUM THEORETICAL 694 Hz 107 kPa

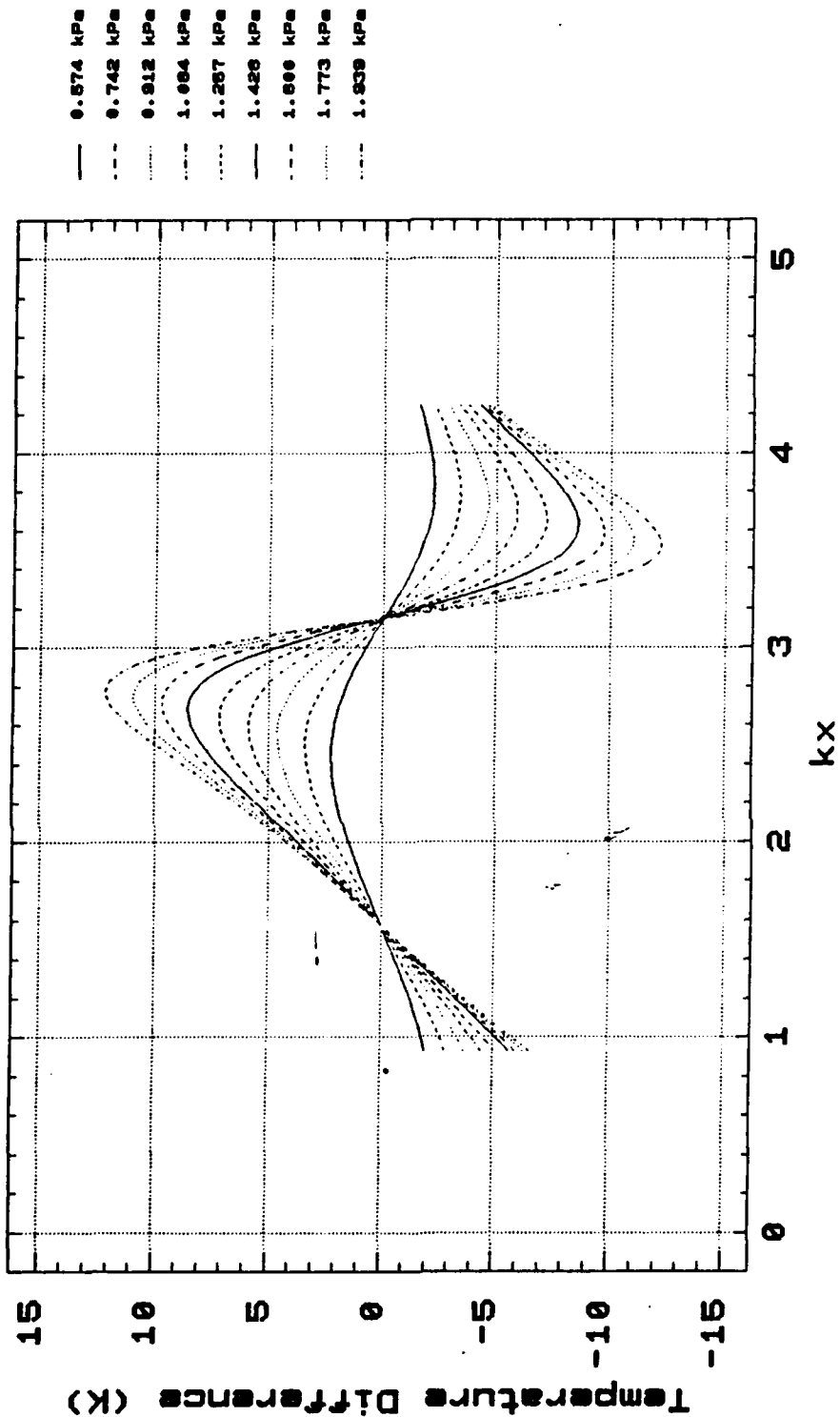


Figure 22

Series 4a Increasing Frequency

HELIUM EXPERIMENTAL 694 Hz 107 kPa

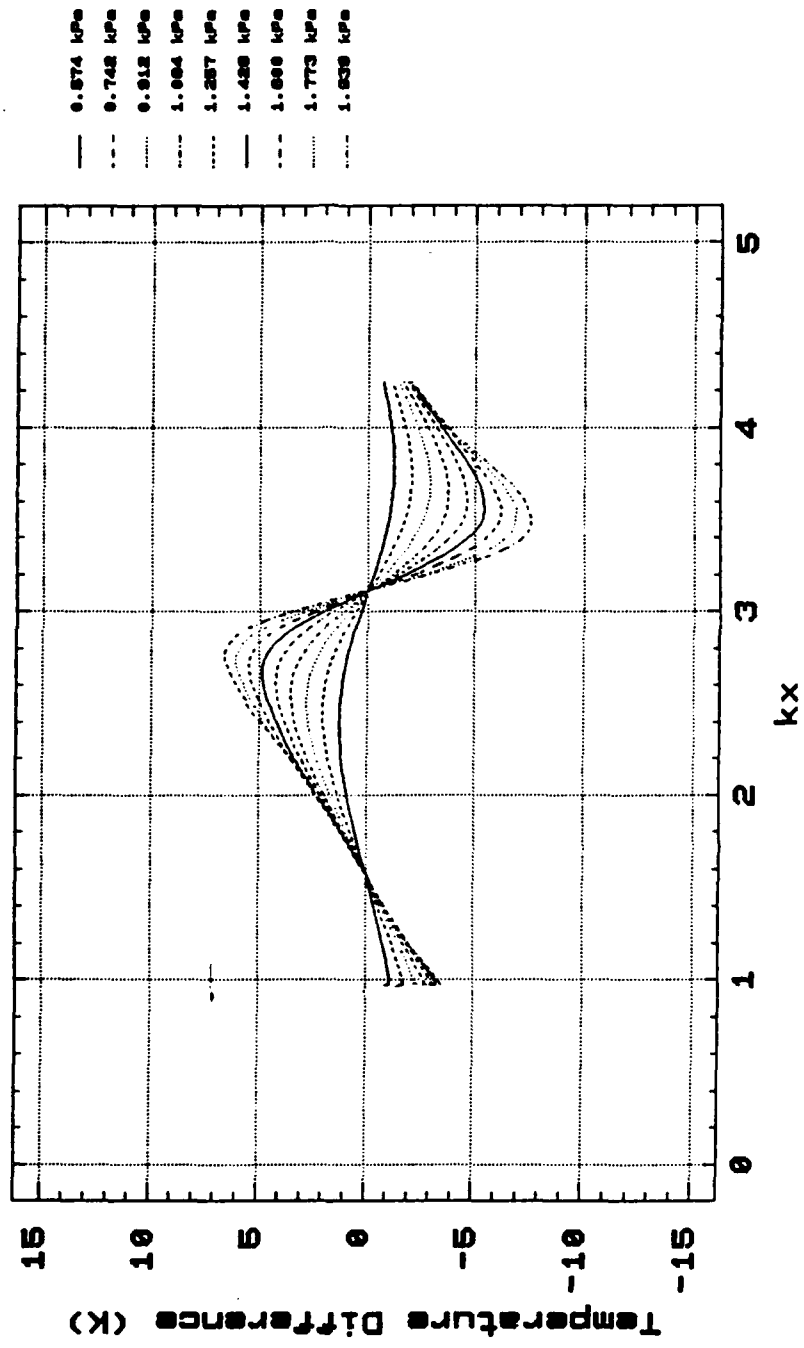


Figure 23
Series 4b Increasing Frequency

HELIUM EXPERIMENTAL 1077 Hz 107 kPa

Temperature Difference (K)

Series 4c Increasing Frequency

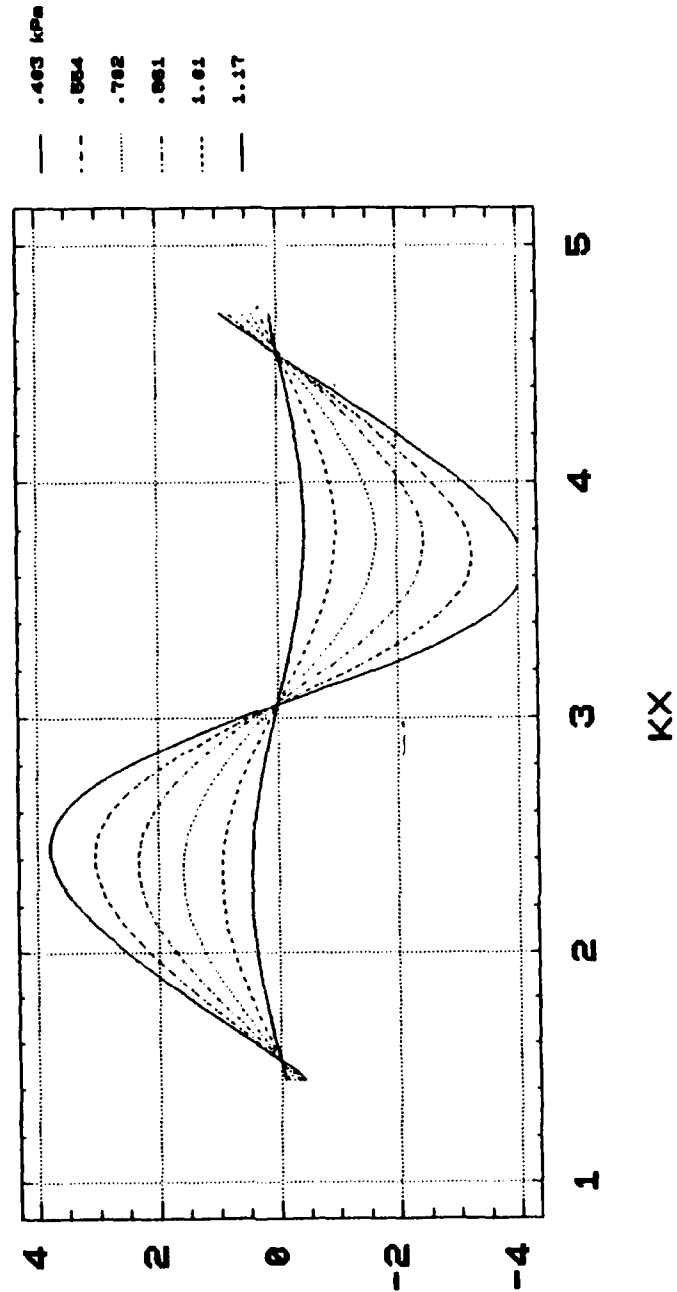
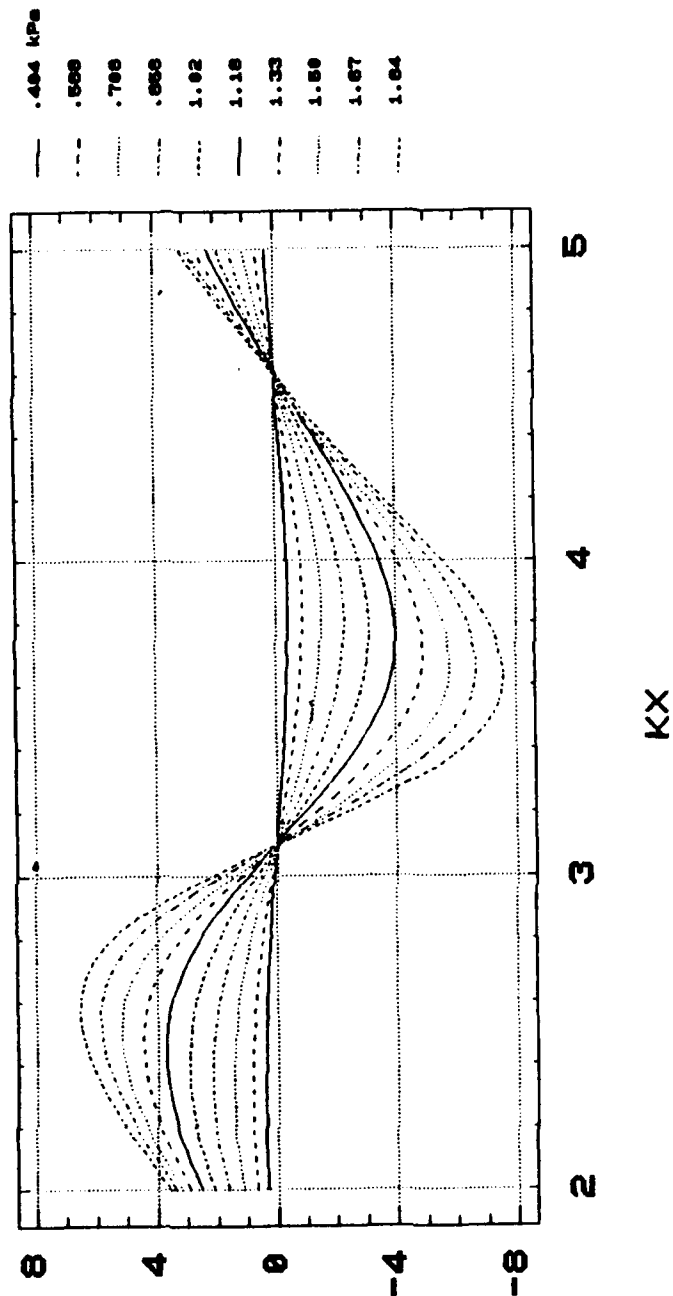


Figure 24

HELIUM EXPERIMENTAL 1464 Hz 107 kPa

Temperature Difference (K)

Figure 25
Series 4d Increasing Frequency



HELIUM EXPERIMENTAL 1860 Hz 107 kPa

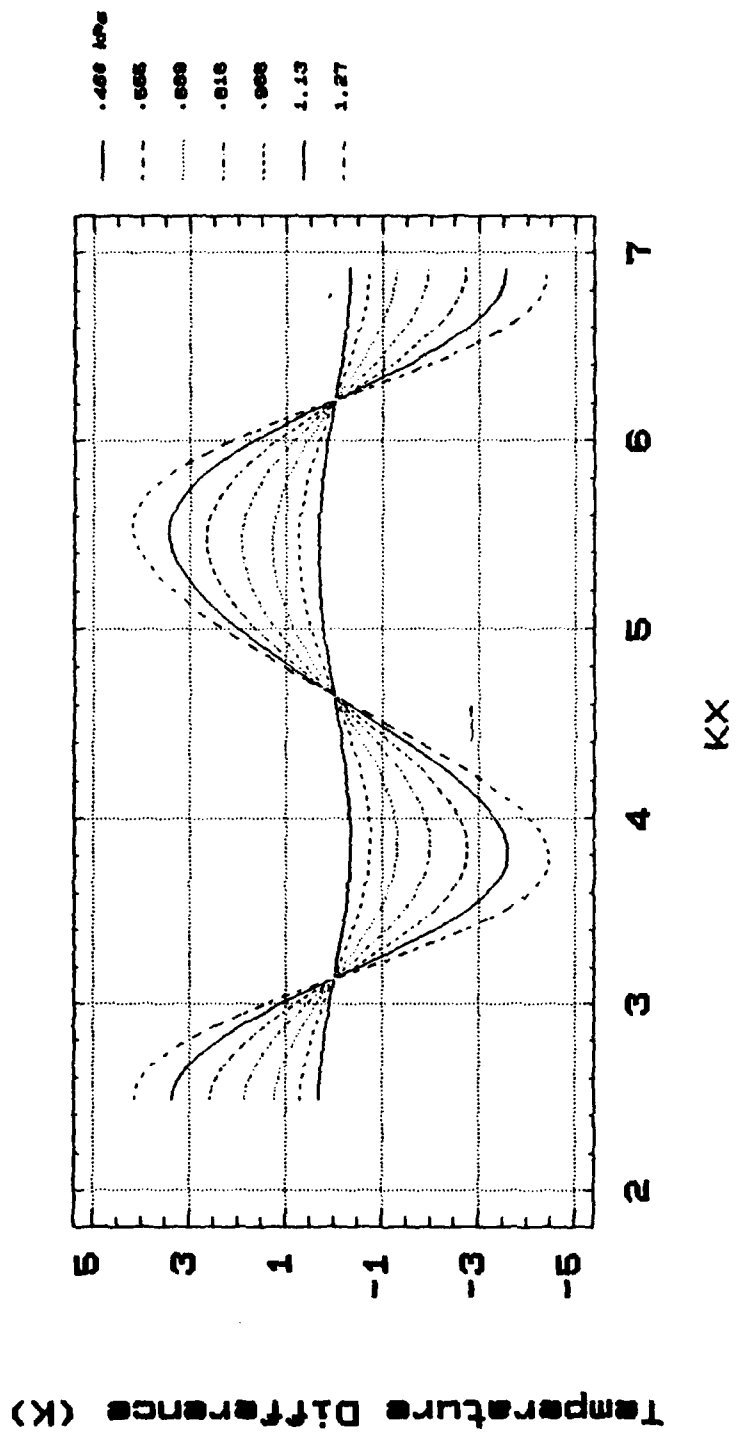


Figure 26
Series 4e Increasing Frequency

(KX in multiples of $n\pi$) and degradation at the pressure nodes (KX at $(2n+1)(\pi/2)$). Similar skewing to what he showed was also evident.

A second feature present in all of the series was an asymmetry in the magnitude of the maximum temperature differences. The magnitude of the positive temperature difference ($T_H - T_C$) was always less than that of the negative ($T_C - T_H$) difference.

The shape of the curves also exhibited interesting properties. The curve shape was remarkably similar from cycle to cycle on the same side of the ΔT axis, but varied greatly from above to below the axis.

Examination of the maximum temperature differences vs pressure amplitude (Figure 27) reveals the rate at which the temperature difference falls off as the acoustic and mean pressure increases. Several of the data sets start to show a saturation of the effect at high acoustic and mean or static pressures.

MAXIMUM TEMP. DIFF. vs PRESSURE AMPL.

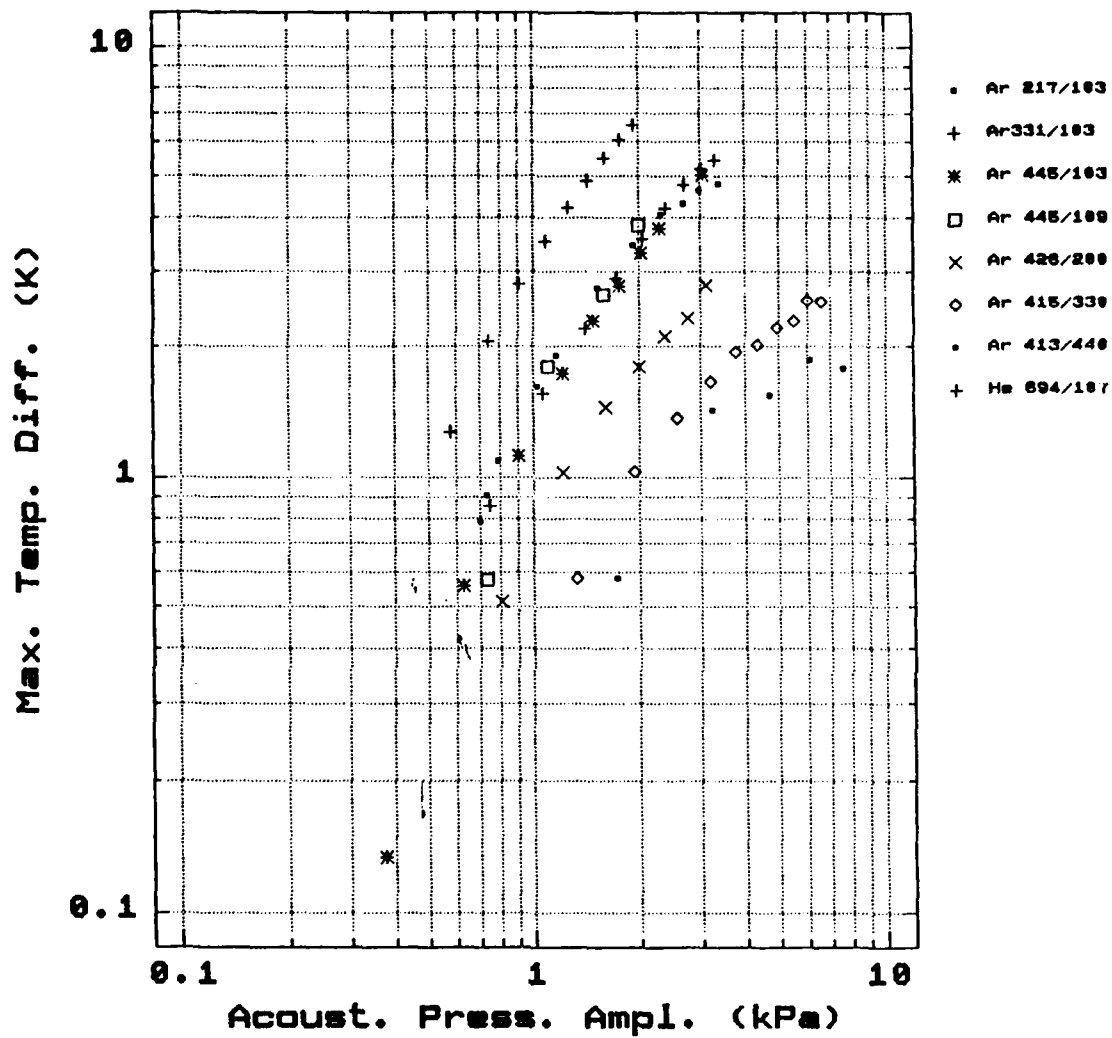


Figure 27
Maximum Temperature Difference vs Pressure Amplitude

V. SUMMARY/RECOMMENDATIONS

The main accomplishment of this thesis was to put together a system enabling computerized measurement of temperature gradients developed across short plates by thermoacoustic heat transport. Measurements were made of the gradients under different static and acoustic pressures, different frequencies, and different gases. Comparison with theoretical values showed results similar to those found by Muzzerall and further showed a gradual degradation of agreement from low to high acoustic pressures. The thermoacoustic effect becomes saturated at the higher values of acoustic pressure amplitude. Also, theoretical values and measured data diverge most severely in the area of pressure nodes. The causes of both of these effects bear further investigation.

LIST OF REFERENCES

1. Wheatley, J.T., Hofler, T., Swift, G., and Migliori, A., "Understanding Some Simple Phenomena in Thermoacoustics with Applications to Acoustical Heat Engines", *American Journal of Physics*, v. 53, pp. 147-162, February 1985.
2. Wheatley, J.T., Hofler, T., Swift, G., and Migliori, A., "An Intrinsically Irreversible Thermoacoustic Heat Engine", *Journal of the Acoustical Society of America*, v. 74(1), July 1983.
3. Muzzerall, M.L., *Investigation of Thermoacoustic Heat Transport Using a Thermoacoustic Couple*, Master's Thesis, Naval Postgraduate School, Monterey, California, September 1987.
4. Swift, G.W., "Thermoacoustic Engines", *Journal of the Acoustical Society of America*, v. 84, pp. 1145-1180, October 1988.

INITIAL DISTRIBUTION LIST

	<u>No. Copies</u>
1. Defense Technical Information Center Cameron Station Alexandria, VA 22304-6145	2
2. Library, Code 0142 Naval Postgraduate School Monterey, CA 93943-5002	2
3. Department Chairman, Code 61 Naval Postgraduate School Monterey, CA 93943	1
4. Dr. L. E. Hargrove Office of Naval Research Physics Division - Code 1112 800 North Quincy Street Arlington, VA 22217	1
5. Dr. G. W. Swift Condensed Matter & Thermal Physics (P-10) Los Alamos National Laboratory P. O. Box 1667/MS 764 Los Alamos, NM 87545	1
6. Professor A. Atchley, Code 61Ay Naval Postgraduate School Monterey, CA 93943	5
7. Dr. T. J. Hofler, Code 61Hf Naval Postgraduate School Monterey, CA 93943	1
8. Professor S. Garrett, Code 61Gx Naval Postgraduate School Monterey, CA 93943	1
9. Captain Michael Muzzerall 301 Daniel Place Victoria, British Columbia CANADA V9C 1W2	1
10. National Center for Physical Acoustics ATTN: NCPA Librarian University of Mississippi University, MS 38677	1

- | | | |
|-----|--|---|
| 11. | Dr. Henry E. Bass | 1 |
| | Physical Acoustics Research Laboratory | |
| | University of Mississippi | |
| | University, MS 38677 | |
| 12. | LCDR M. D. Kite | 2 |
| | 709 Bruce Court | |
| | Herndon, VA 22070 | |